V2(a) Graph Basics – needed for assignments 1 & 2

A **graph** *G* is an ordered pair *(V, E)* of a set *V* of **vertices** and a set *E* of **edges**.

Degree distribution *P(k)*

$$P(k) = \frac{n_k}{N}$$

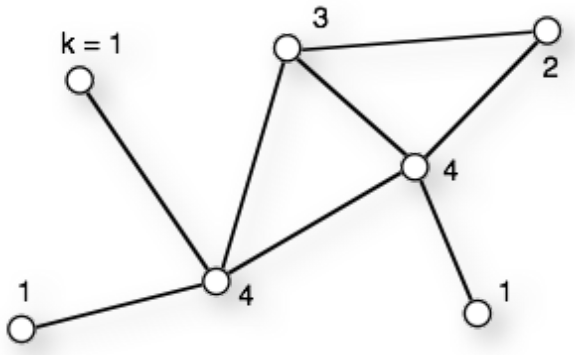

k	0	1	2	3	4
P(k)	0	3/7	1/7	1/7	2/7

Random network:

also called the "Erdös-Renyi model“:

- start with set of given nodes
- then add links randomly

P(k) = "Poisson“ (will show this on the next slides)

$$P(k) = \frac{\lambda^k}{k!} e^{-\lambda}$$

Connected Components

Connected graph <=> there is a path between all pairs of nodes

In large (random) networks: complete $\{V\}$ is often not connected
→ identify connected subsets $\{V_i\}$ with $\{V\} = \cup \{V_i\}$
→ **connected components** (CC)

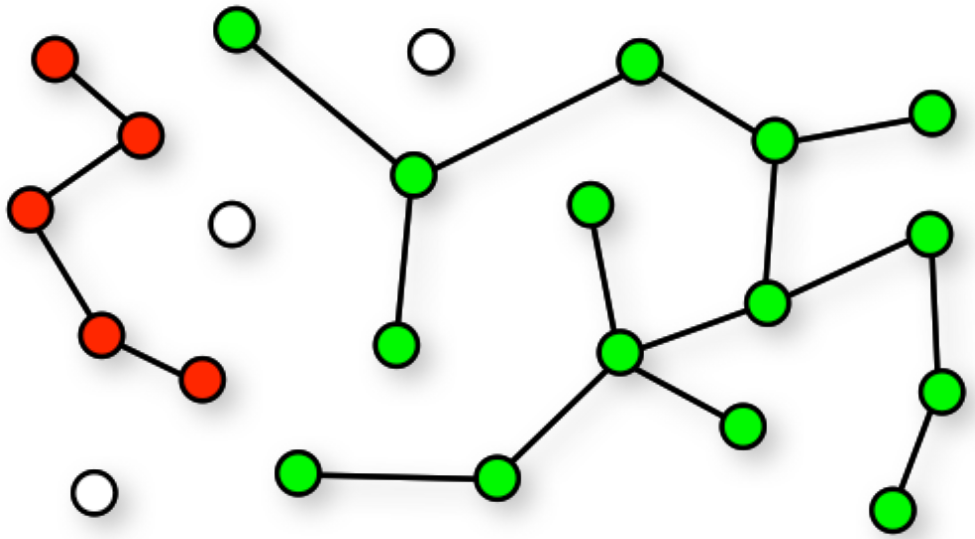

#CC = 5
N_{max} = 15
N_{min} = 1

Connectivity of the Neighborhood

How many of the neighboring vertices are themselves neighbors?
=> this is measured by the **clustering coefficient** *C(k)*

Number of possible undirected edges between *k* nodes: $n_{max} = \frac{k\,(k-1)}{2}$

n_k is the actual number of edges between the neighbor nodes.

Fraction of actual edges ≅ **clustering coefficient** $C(k, n_k) = \frac{2n_k}{k\,(k-1)}$

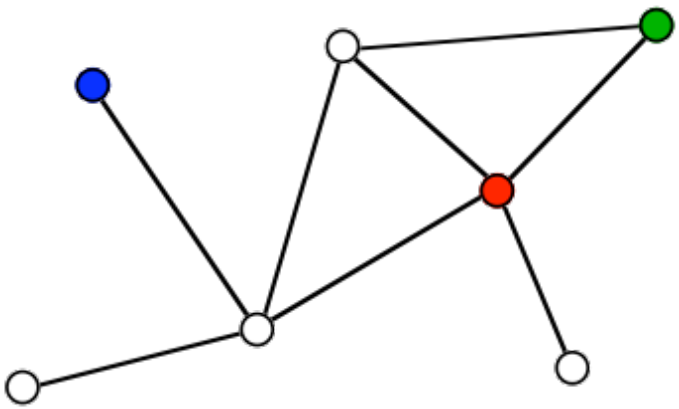

green: $k = 2,\ n_k = 1 \rightarrow C = 1$

red: $k = 4,\ n_k = 2 \rightarrow C = 1/3$

blue: $k = 1,\ n_k = ? \rightarrow$ C is not defined

Note: clustering coeff. is sometimes also defined via fraction of possible triangles

Clustering Coefficient of a Graph

Data: C_i for each node i $\rightarrow$ N values

Statistics:

average at **fixed k**

$$\rightarrow \quad C(k) = \frac{1}{n_k} \sum_{k_i = k} C_i$$

average over **all nodes**

$$\rightarrow \quad \langle C \rangle = \frac{1}{N} \sum C_i$$

Note: it is also possible to average the *C(k)*
$\Rightarrow$ This yields a different value for <*C*> !!!
because no weighting is done for different occupancy of k's.

Basic Types: (1) Random Network

Generally: *N* vertices connected by *L* edges

More specific: **distribute** the edges **randomly** between the vertices

Maximal number of links between *N* vertices:

$$L_{max} = \frac{N(N-1)}{2}$$

=> **probability** *p* for an edge between two randomly selected nodes:

$$p = \frac{L}{L_{max}} = \frac{2L}{N(N-1)}$$

=> **average degree** λ

$$\lambda = \frac{2L}{N} = p\,(N-1)$$

path lengths in a random network grow with `ln`(*N*) => **"small world"**

Random Network: *P(k)*

Network with *N* vertices, *L* edges
=> probability for a random link:

$$p = \frac{2L}{N(N-1)}$$

Probability that random node has links to *k* other particular nodes:

$$W_k = p^k (1-p)^{N-k-1}$$

Probability that random node has links to any *k* other nodes:

$$P(k) = \binom{N-1}{k} W_k = \frac{(N-1)!}{(N-k-1)!\,k!} W_k$$

Limit of large graph: $N \to \infty$, $p = \lambda / N$

$$\begin{aligned}
\lim_{N\to\infty} P(k) &= \lim_{N\to\infty} \frac{N!}{(N-k)!\,k!} p^k (1-p)^{N-k} \\
&= \lim_{N\to\infty} \left(\frac{N(N-1)\dots(N-k+1)}{N^k}\right) \frac{\lambda^k}{k!} \left(1-\frac{\lambda}{N}\right)^N \left(1-\frac{\lambda}{N}\right)^{-k} \\
&= \qquad 1 \qquad\qquad \frac{\lambda^k}{k!} \qquad \mathrm{e}^{-\lambda} \qquad\quad 1 \\
&= \frac{\lambda^k}{k!} \mathrm{e}^{-\lambda}
\end{aligned}$$

Random Network: *P(k)*

Many independently placed edges => **Poisson statistics**

$$P(k) = \frac{\lambda^k}{k!} e^{-\lambda}$$

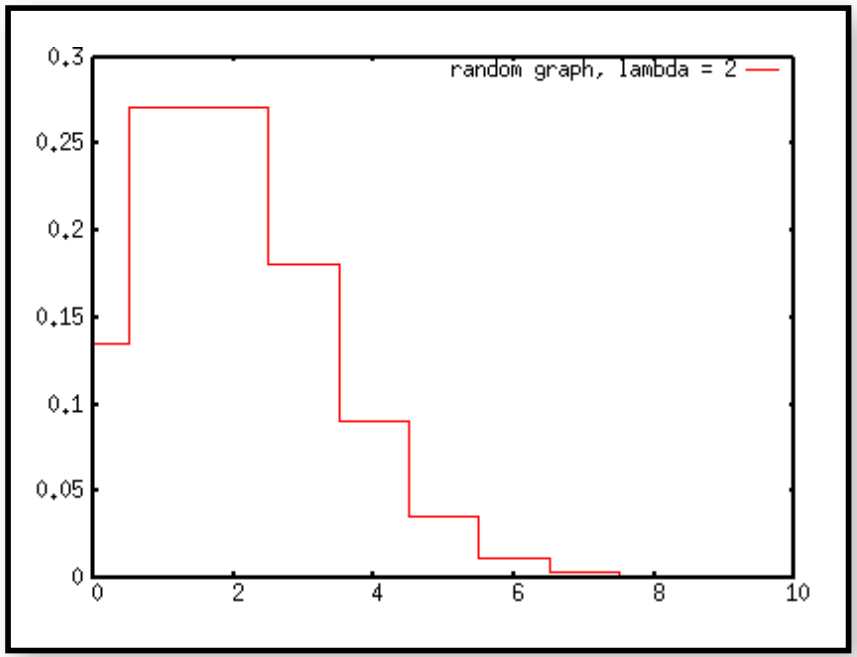

k	*P(k / λ = 2)*
0	0.14
1	0.27
2	0.27
3	0.18
4	0.090
5	0.036
6	0.012
7	0.0034
8	0.00086
9	0.00019
10	3.82e-05

=> Small probability for $k >> \lambda$

Basic Types: (2) Scale-Free

Growing network a la Barabasi and Albert (1999):

- start from a small "nucleus“ of m_0 connected nodes
- add new node with n links
- connect new links to existing nodes with probability p_i proportional to degree k_i of each existing node (“preferential attachment”);

=> "the rich get richer" $$p_i = \left(\frac{k_i}{\sum k_i} \right)^{\beta}$$ in BA-model β = 1

Properties:

- this leads to a power-law degree distribution:

$$P(k) \propto k^{-\gamma}$$ with γ = 3 for the BA model

- self-similar structure with highly connected hubs (no intrinsic length scale)

=> average path length grows with `ln` (N) / `ln`(`ln`(*N*))

=> this grows much slower than for random graphs

=> **“very small world”**

The Power-Law Signature

Power law $$P(k) \propto k^{-\gamma}$$

Take log on both sides:

$$\log(P(k)) = -\gamma \log(k)$$

Plot log(*P*) vs. log(*k*) => straight line

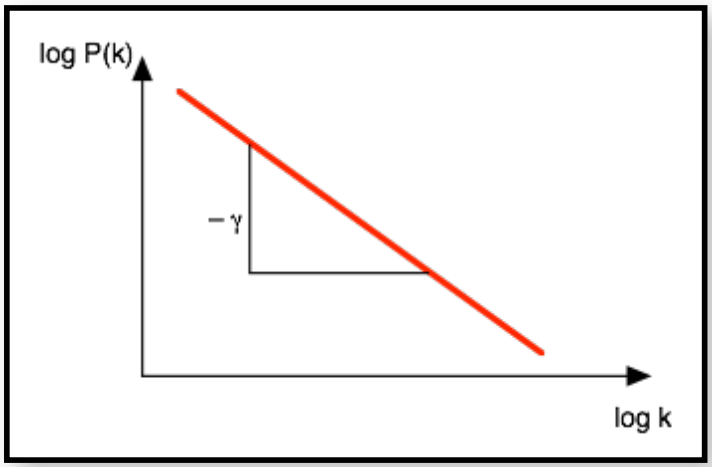

Note: for fitting γ against experimental data it is often better to use the integrated *P(k)*
=> integral smoothes the data

$$\int_{k_0}^{k} P(k)dk = \left[-\frac{k^{-(\gamma-1)}}{\gamma}\right]_{k_0}^{k}$$

Scale-Free: Examples

The World-Wide-Web:

=> growth via links to portal sites

Flight connections between airports

=> large international hubs, small local airports

Protein interaction networks

=> some central,

ubiquitous proteins

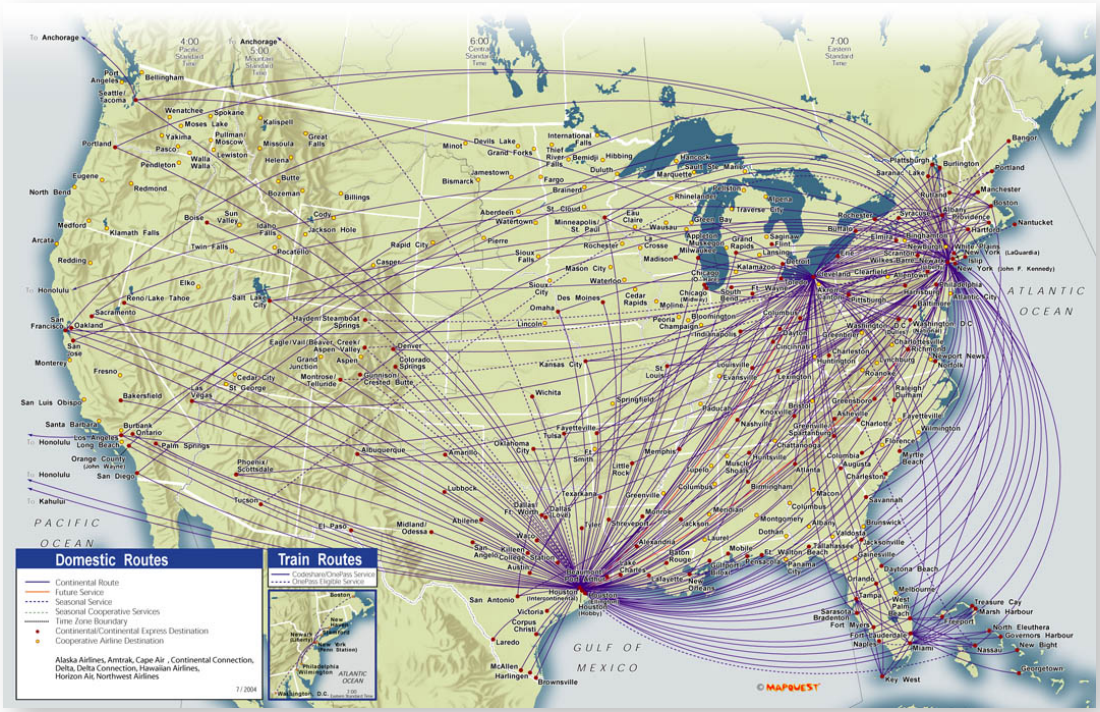

http://a.parsons.edu/~limam240/blogimages/16_full.jpg

Hierarchical, Regular, Clustered…

Tree-like network with similar degrees
=> like an organigram
=> hierarchic network

All nodes have the same degree
and the same local neighborhood
=> regular network

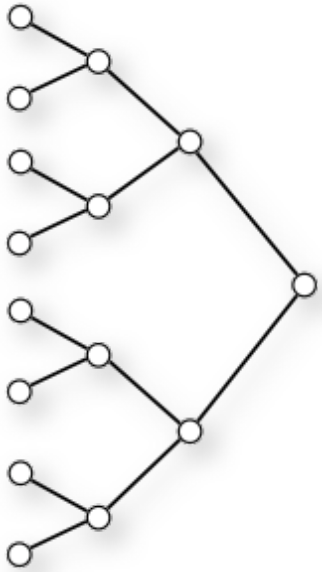

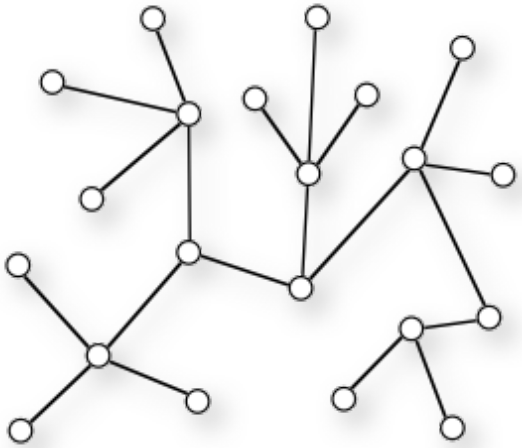

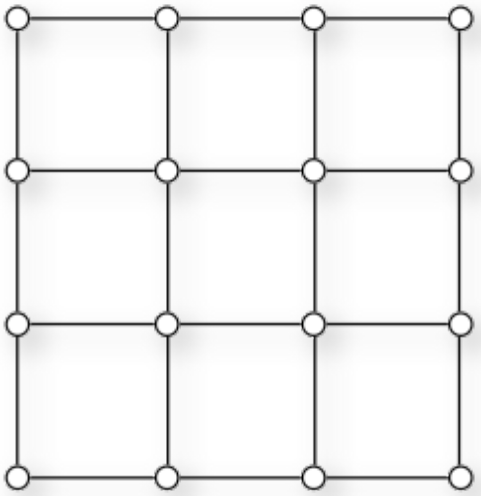

P(k) for these example networks? (finite size!)

Note: most real-world networks are somewhere in between the basic types

C(k) for a Random Network

Clustering coefficient when *m* edges exist between *k* neighbors

$$C(k,m) = \frac{2m}{k(k-1)}$$

Probability to have exactly *m* edges between the *k* neighbors

$$W(m) = \binom{k}{m} p^m (1-p)^{\frac{k(k-1)}{2}-m}$$

In this way, we pick the *m* start nodes for the *m* edges from the *k* nodes.

Average *C(k)* for degree *k*:

$$C(k) = \frac{\sum_{m=0}^{\frac{k(k-1)}{2}} W(m)\, C(k,m)}{\sum_{m=0}^{\frac{k(k-1)}{2}} W(m)} = \ldots = p$$

→ *C(k)* is independent of *k*
<=> same local connectivity throughout the network

Clusters in scale free graphs

Scale-free network <=> no intrinsic scale

→ same properties at any *k*-level

→ same local connectivity

→ *C(k)* = const.

"Real" biological data

→ missing links

→ multiple clusters

Is the metabolic network of a cell fully connected?

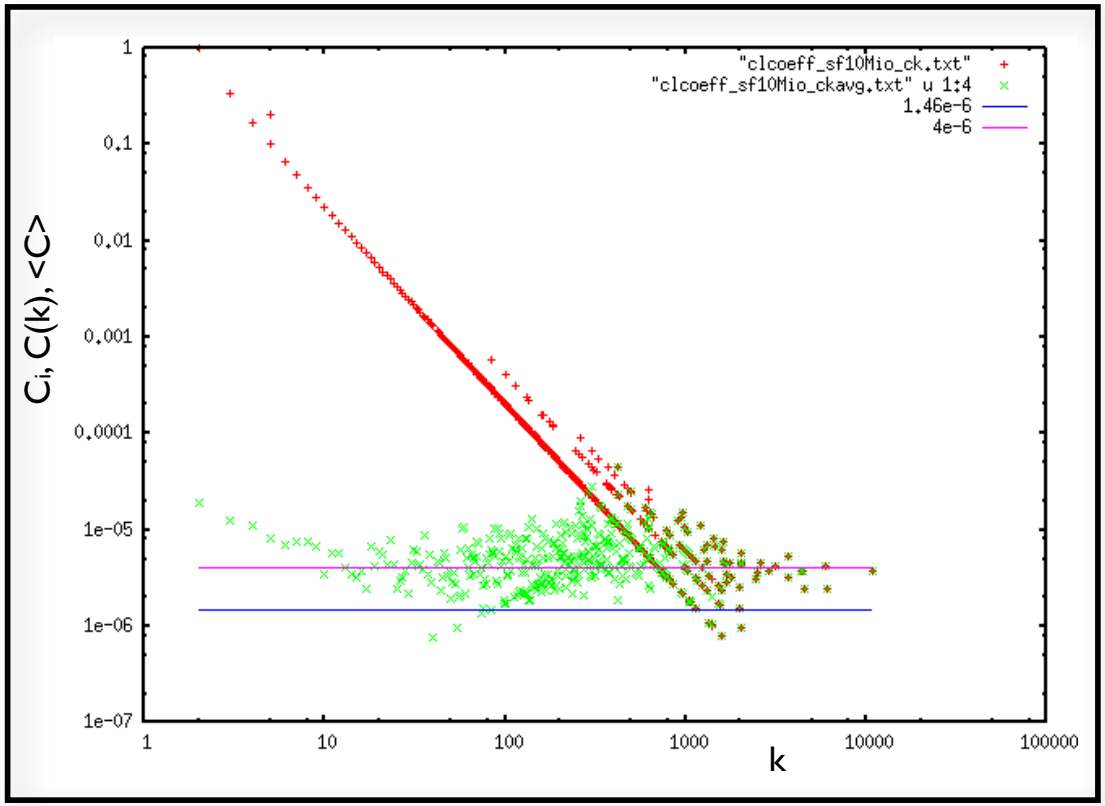

Algorithms on Graphs

How to **represent** a graph in the **computer**?

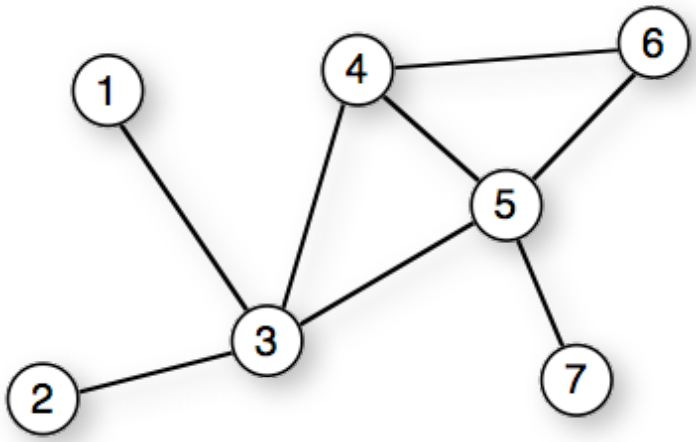

1. **Adjacency list**

=> list of neighbors for each node

1: (3)
2: (3)
3: (1, 2, 4, 5)
4: (3, 5, 6)
5: (3, 4, 6, 7)
6: (4, 5)
7: (5)

+ minimal memory requirement
+ vertices can easily be added or removed

– requires $O(\lambda)$ time to determine whether a certain edge exists

Note: for weighted graphs store pairs of (neighbor label, edge weight)

Graph Representation II

2. **Adjacency matrix** (see V1)

→ N x N matrix with entries M_{uv}

M_{uv} = weight when edge between u and v exists,
0 otherwise

→ symmetric for undirected graphs

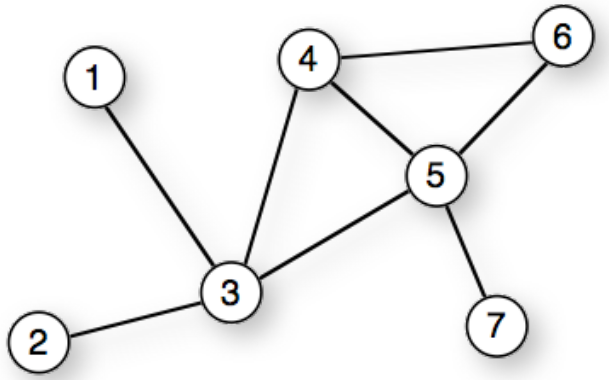

	1	2	3	4	5	6	7
1	–	0	1	0	0	0	0
2	0	–	1	0	0	0	0
3	1	1	–	1	1	0	0
4	0	0	1	–	1	1	0
5	0	0	1	1	–	1	1
6	0	0	0	1	1	–	0
7	0	0	0	0	1	0	–

+ fast *O(1)* lookup of edges
– large memory requirements
– adding or removing nodes is expensive

Note: very convenient in programming languages that support sparse multi-dimensional arrays
=> Perl

Graph Representation III

3. **Incidence matrix**

→ *N* x *M* matrix with entries M_{nm}

M_{nm} = weight when edge *m* ends at node *n*

0 otherwise

→ for a plain graph there are two entries per column

→ directed graph:
indicate direction via sign (in/out)

The incidence matrix is a special form of the stoichiometric matrix of reaction networks.

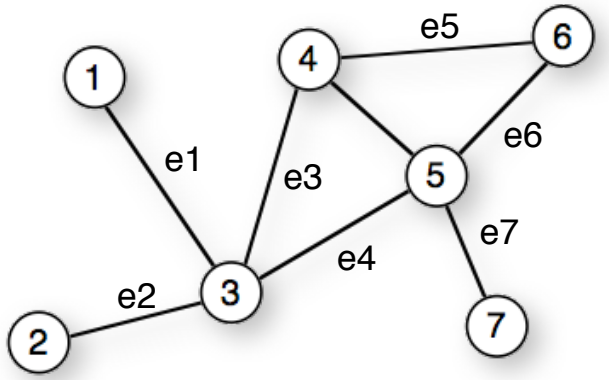

	e1	e2	e3	e4	e5	e6	e7
1	1						
2		1					
3	1	1	1	1			
4			1		1		
5				1		1	1
6					1	1	
7							1

V2(b): Structures of Protein Complexes and Subcellular Structures

(1) We normally assume that various enzymes of a biochemical pathway „swim“ in the cytosol and randomly meet the substrate molecules one after another.

Yet, sometimes **multiple enzymes** of a biochemical pathway associate into **large complexes** and „hand over“ the substrates from one active site to the next one.

Advantage: this avoids free diffusion, increases local substrate density.

(2) Membrane transporters and receptors often form **oligomers** in the **membrane**.

Advantage:

(i) large structures are built from small building blocks (simplicity)

(ii) Oligomer formation can be regulated separately from transcription.

(3) Also: complicated structural components of the cell (e.g. cytoskeleton) are built from many small components (e.g. actin)

2.1 RNA Polymerase II

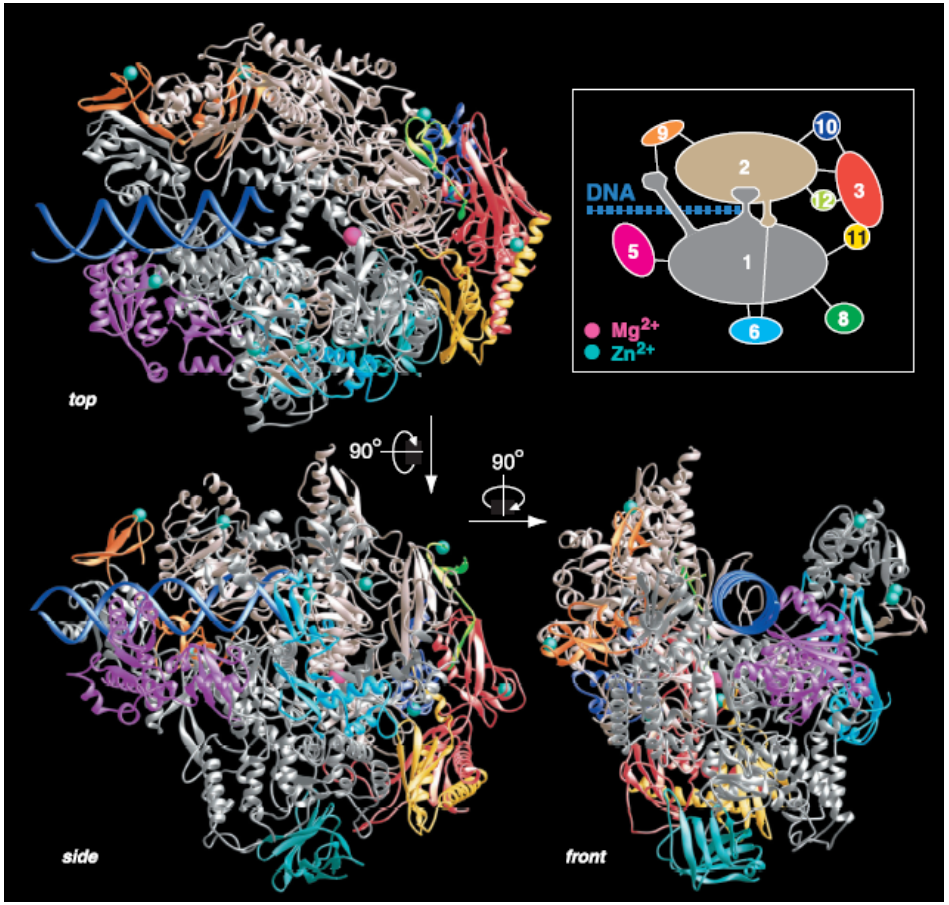

RNA polymerase II is the central enzyme of gene expression and synthesizes all messenger RNA in eukaryotes.

Cramer *et al.,* Science 288, 640 (2000)

2.1 RNA processing: splicesome

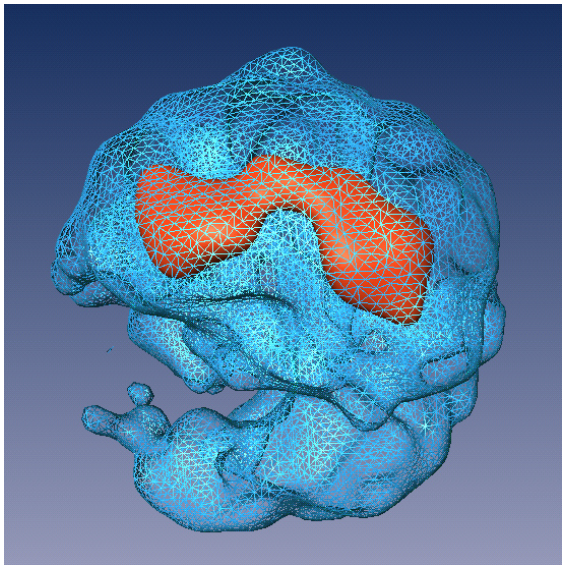
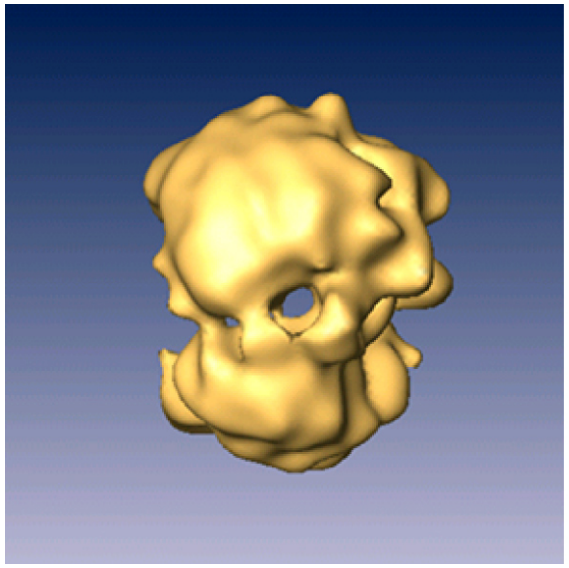
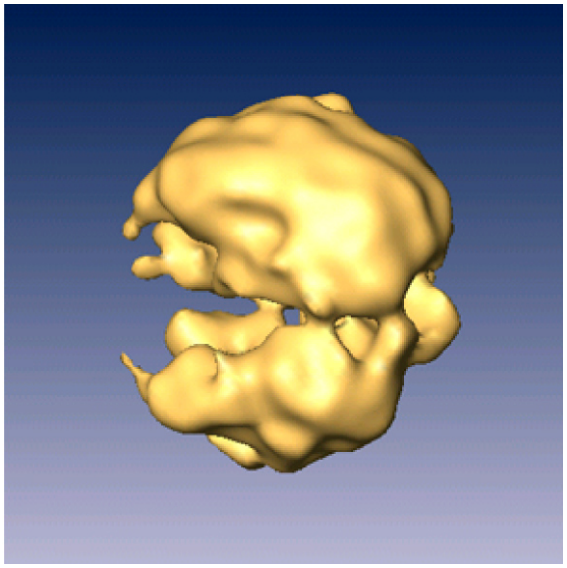

Structure of a **cellular editor** that "cuts and pastes" the first draft of RNA straight after it is formed from its DNA template.

It has two distinct, unequal halves surrounding a tunnel.

Larger part: appears to contain proteins and the short segments of RNA, smaller half: is made up of proteins alone.

On one side, the tunnel opens up into a cavity, which is believed to function as a holding space for the fragile RNA waiting to be processed in the tunnel.

Profs. Ruth and Joseph Sperling, http://www.weizmann.ac.il/

2.1 Protein synthesis: ribosome

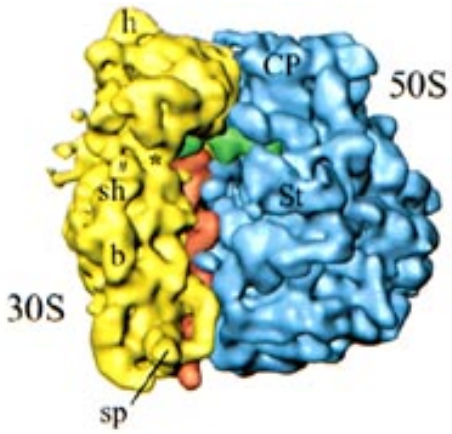

The ribosome is a complex subcellular particle composed of protein and RNA. It is the site of protein synthesis,

http://www.millerandlevine.com/chapter/12/cryo-em.html

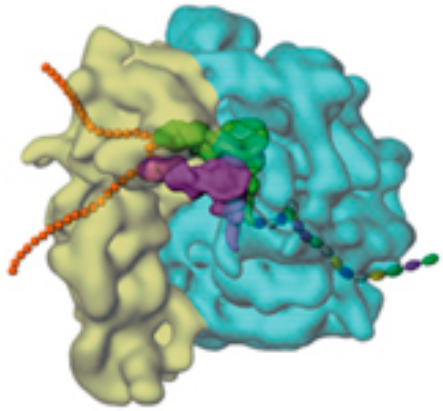

Model of a ribosome with a newly manufactured protein (multicolored beads) exiting on the right.

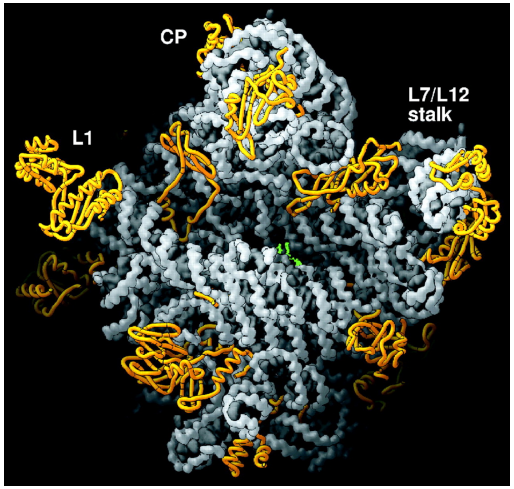

large ribosomal subunit from *Haloarcula marismortui*. RNA is shown in gray and the protein backbone in yellow.
Ban *et al.* (2000)

Components of ribosome assemble spontaneously in vitro: no helper proteins (assembly chaperones) needed

2.1 Nuclear Pore Complex (NPC)

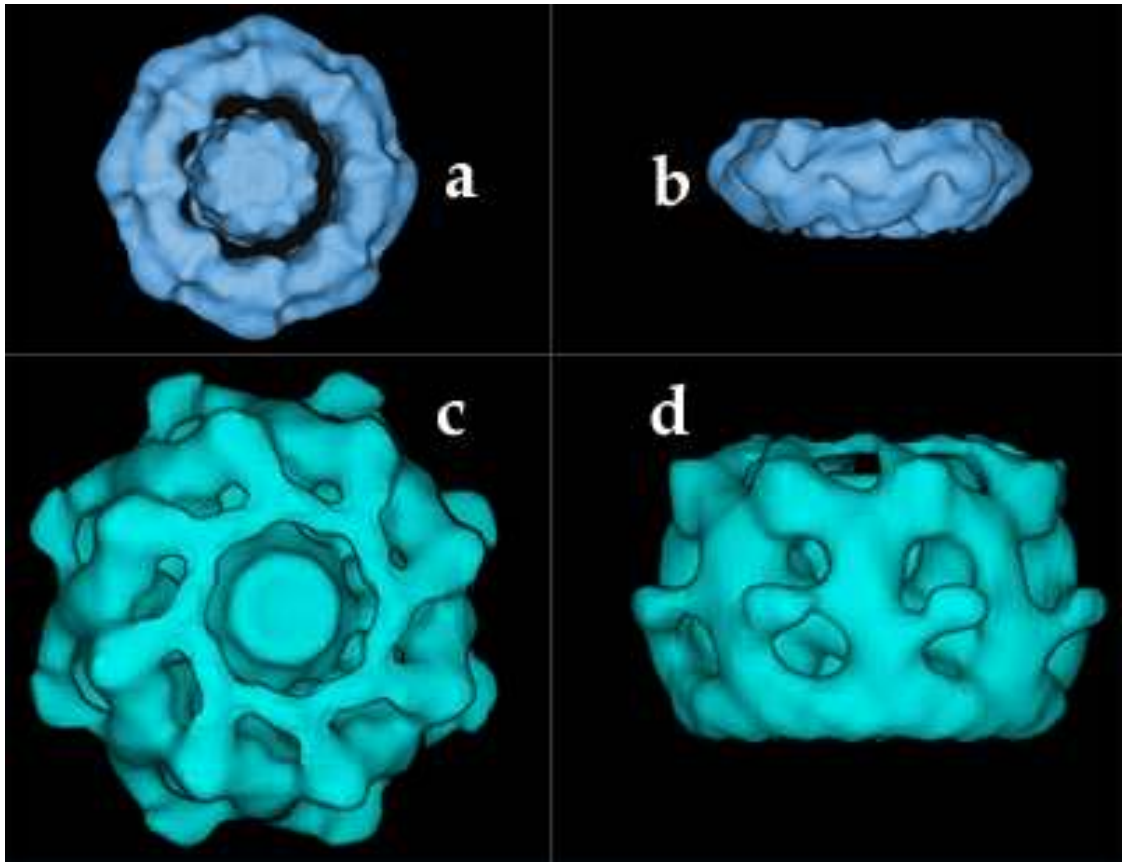

Three-dimensional image of the NPC obtained by electron microscopy.
A-B The NPC in yeast.
Figure A shows the NPC seen from the cytoplasm while figure B displays a side view.

C-D The NPC in vertebrate (Xenopus).

http://www.nobel.se/medicine/educational/dna/a/transport/ncp_em1.html
Three-Dimensional Architecture of the Isolated Yeast Nuclear Pore Complex: Functional and Evolutionary Implications, Qing Yang, Michael P. Rout and Christopher W. Akey. Molecular Cell, 1:223-234, 1998

NPC is a 50-100 MDa protein assembly that regulates and controls trafficking of macromolecules through the nuclear envelope.

Molecular structure: lecture V20

2.1 Arp2/3 complex

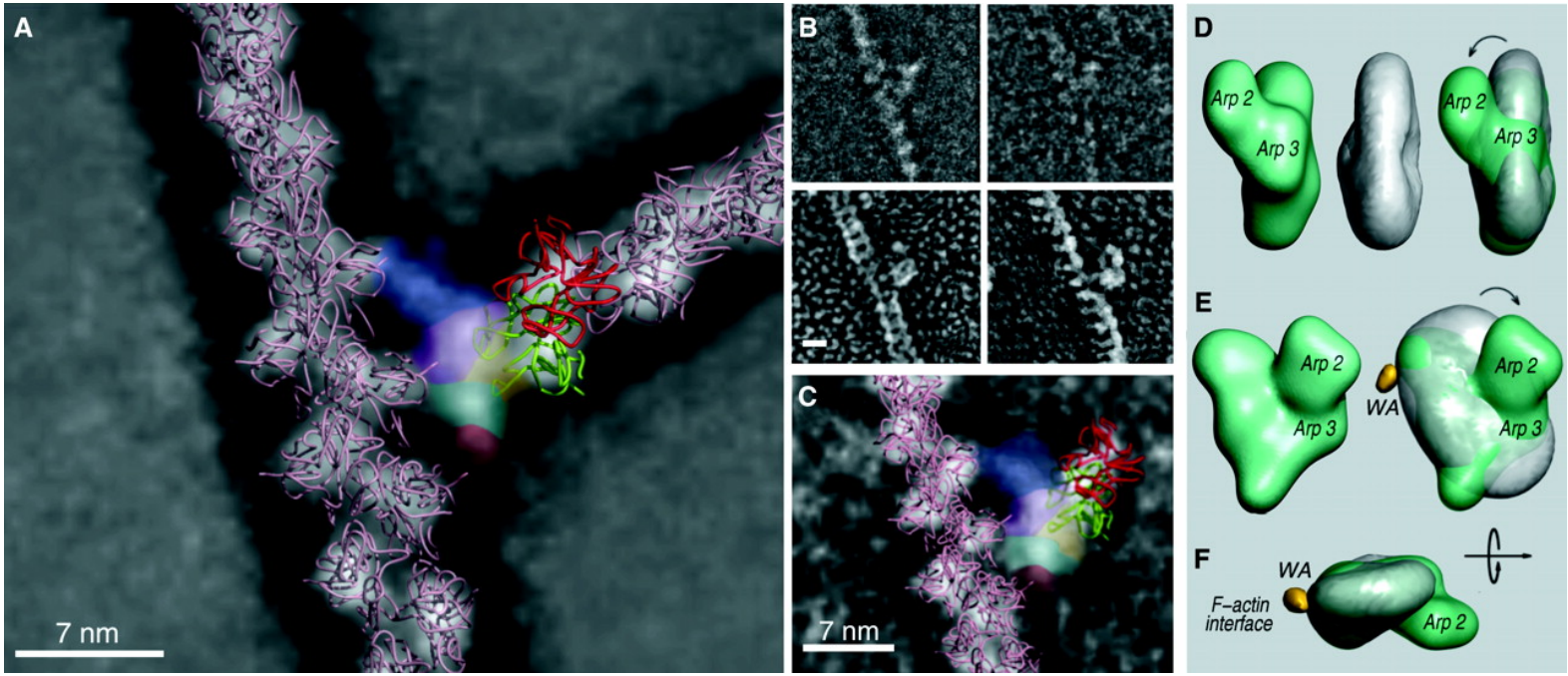

The seven-subunit Arp2/3 complex choreographs the formation of branched actin networks at the leading edge of migrating cells.
(A) Model of actin filament branches mediated by *Acanthamoeba* Arp2/3 complex.
(D) Density representations of the models of actin-bound (green) and the free, WA-activated (as shown in Fig. 1D, gray) Arp2/3 complex.

Volkmann *et al.,* Science 293, 2456 (2001)

2.1 icosahedral pyruvate dehydrogenase complex: a multifunctional catalytic machine

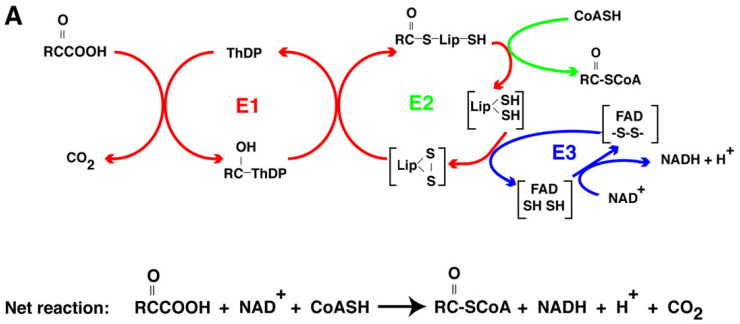

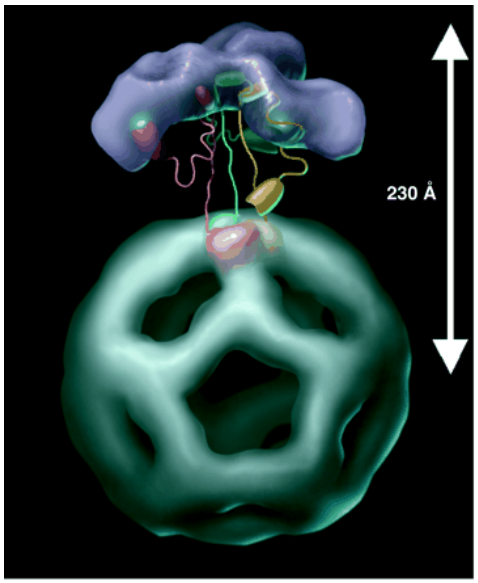

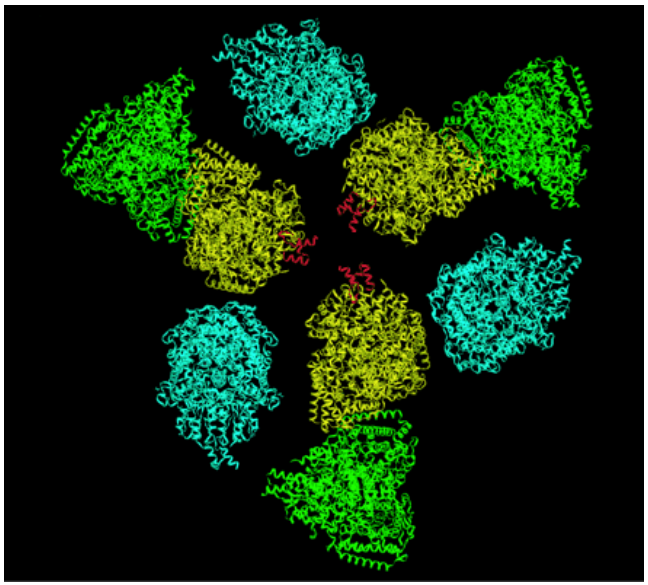

Milne *et al.,* EMBO J. 21, 5587 (2002)

Model for active-site coupling in the E1E2 complex. 3 E1 tetramers (purple) are shown located above the corresponding trimer of E2 catalytic domains in the icosahedral core. Three full-length E2 molecules are shown, colored red, green and yellow. The lipoyl domain of each E2 molecule shuttles between the active sites of E1 and those of E2. The lipoyl domain of the red E2 is shown attached to an E1 active site. The yellow and green lipoyl domains of the other E2 molecules are shown in intermediate positions in the annular region between the core and the outer E1 layer. Selected E1 and E2 active sites are shown as white ovals, although the lipoyl domain can reach additional sites in the complex.

2.1 Apoptosome

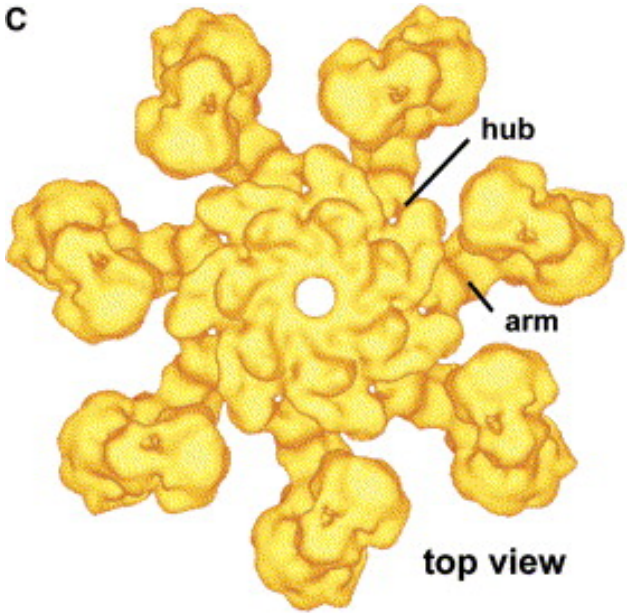

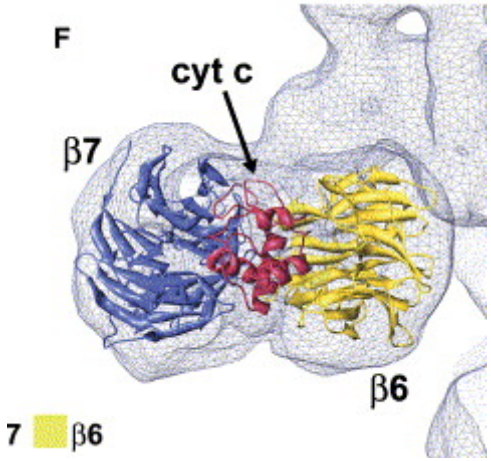

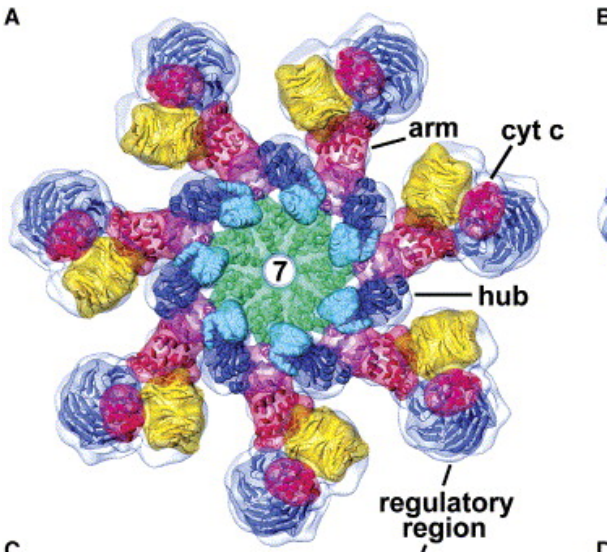

Apoptosis is the dominant form of programmed cell death during embryonic development and normal tissue turnover. In addition, apoptosis is upregulated in diseases such as AIDS, and neurodegenerative disorders, while it is downregulated in certain cancers. In apoptosis, death signals are transduced by biochemical pathways to activate caspases, a group of proteases that utilize cysteine at their active sites to cleave specific proteins at aspartate residues. The proteolysis of these critical proteins then initiates cellular events that include chromatin degradation into nucleosomes and organelle destruction. These steps prepare apoptotic cells for phagocytosis and result in the efficient recycling of biochemical resources.
In many cases, apoptotic signals are transmitted to mitochondria, which act as integrators of cell death because both effector and regulatory molecules converge at this organelle. Apoptosis mediated by mitochondria requires the release of cytochrome c into the cytosol through a process that may involve the formation of specific pores or rupture of the outer membrane. Cytochrome c binds to Apaf-1 and in the presence of dATP/ATP promotes assembly of the apoptosome. This large protein complex then binds and activates procaspase-9.

2.1.2 Categories of Protein Complexes

Complexes can be classified e.g. by function / size / involvement of other components (nucleic acids, carbohydrates, lipids).

Mechanistic classification:

(1) transient vs. permanent

(2) obligate vs. non-obligate

Obligate: components function only when in the bound state.

Non-obligate: unbound components can also exist as monomers.

Examples: antibodies, signalling complexes, complexes of RNA polymerase with different initiation and elongation factors.

2.3 Determining molecular 3D structures

Experimental techniques:

Dimensions	proteins: 1 – 5 nm	atoms: 0.1 – 0.5 nm
bond stability	covalent ca. 300 kJ/mol	H-bonds: ca. 5 – 20 kJ/mol

X-ray crystallography
NMR
electron microscopy
FRET
AFM pulling

- applicability
- resulting information
- resolution
- distortions
- effort/cost ...

Prediction techniques:

Homology modelling, correlation based fitting, ab-initio modelling

2.3.1 X-ray crystallography

Beam of photons (no mass),
need high energy, method
needs relatively large samples

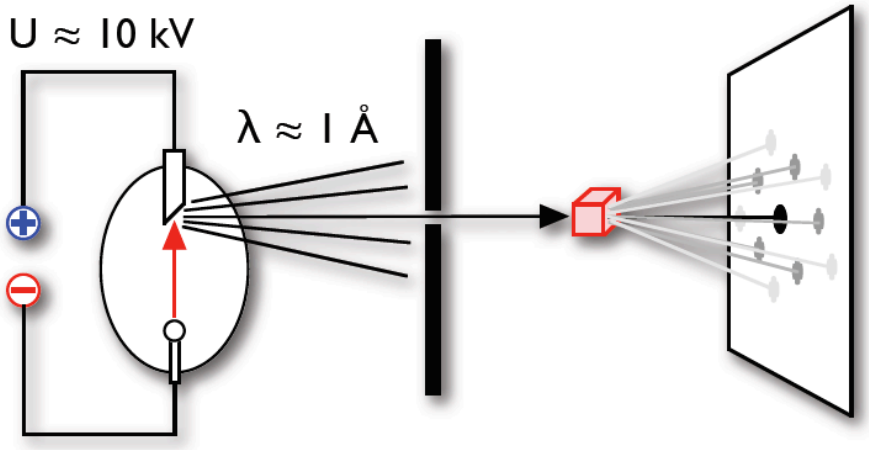

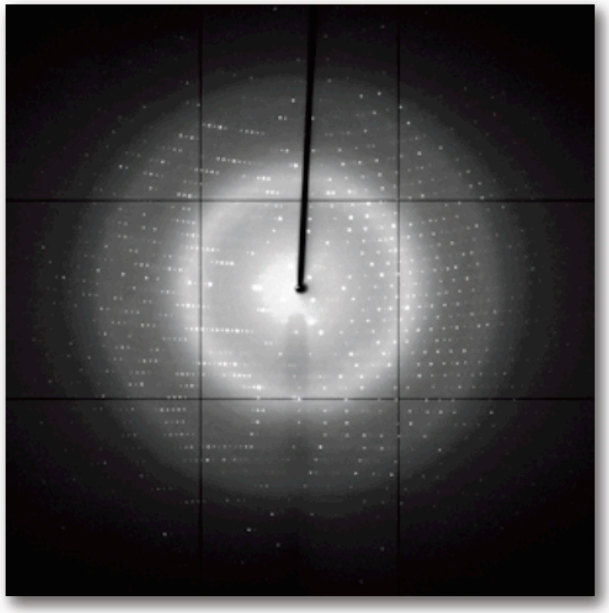

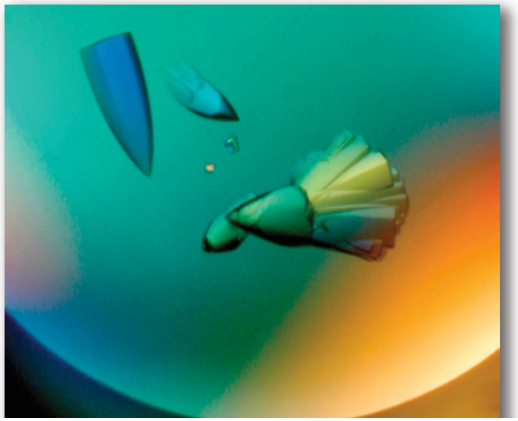

Crystallize proteins, record diffraction patterns
of X-rays (scatter at the electron clouds)
=> reconstruction

1 keV ≈ 10^5 kJ/mol

http://www.molbio1.princeton.edu/macro/about.html

X-ray reconstruction

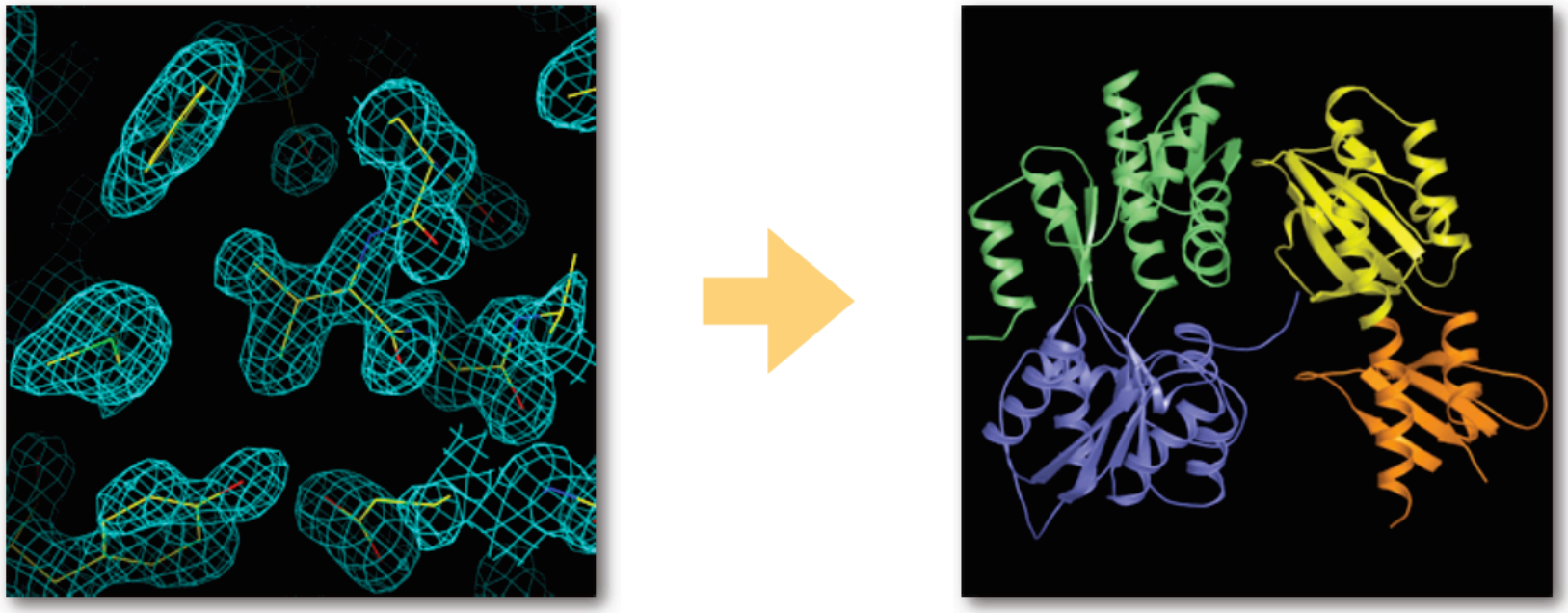

Reconstruct electron density maps from diffraction patterns at multiple wavelengths and orientations, refine structure computationally

Main problem: proteins do not like to crystallize (especially membrane proteins)

PDB: experimental technique == X-Ray: 43138 results
X-Ray && "in the membrane": 1232 results

http://www.molbio1.princeton.edu/macro/about.html

2.3.2 Nuclear magnetic resonance

Place sample with the proteins into strong magnetic field
=> nuclei with non-zero magnetic moment
(^{1}H, ^{13}C, ^{15}N) align

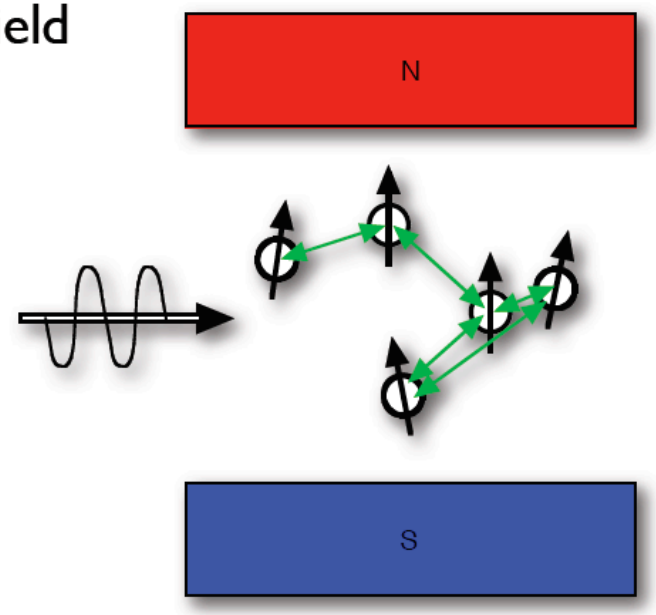

Apply electromagnetic RF field
=> resonances of the nuclear spins depending on
- atom type
- chemical environment

=> extract distances between close by ^{1}H atoms (distance constraints)

\+ no crystallization required, proteins in physiological environment
\+ atomic resolution
– too much overlap for larger proteins (≥ 15 kDa)

2.3.3 Electron microscopy

Like X-ray crystallography, but with electrons (electrons have mass)

=> much stronger interaction with electron clouds

=> works already on 2D crystals (membrane proteins!)

=> strong radiation damage of the sample

=> resolution limited (keep electron energy low) (longer wavelength)

For 3D tomography: rotate sample

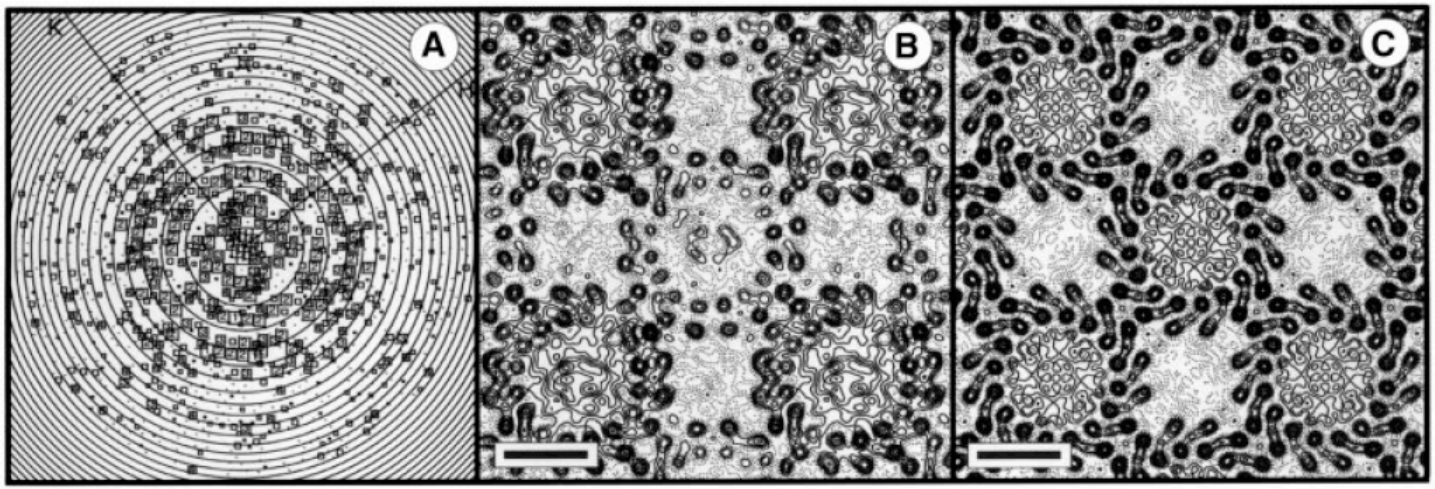

Cryo-EM images of the LH1-RC core complexes of *Rhodospirillum rubrum* at 8.5 Å resolution

Fig. 3. (**A**) Representation of amplitudes of Fourier components calculated for one image of a glucose-embedded tetragonal crystal. Numbers and box sizes correspond to the spot IQ value, with spots of the highest signal-to-noise ratio having an IQ of 1 (Henderson *et al.*, 1986). Spots are shown to a resolution of 1/6 Å^{-1}. (**B**) 8.5 Å resolution projection map calculated from five averaged images of glucose-embedded tetragonal crystals, assuming *p*1 symmetry. Contouring is at 0.5 r.m.s. density with density above mean (protein) represented by solid contours. Scale bar: 50 Å. (**C**) As (B), with $p42_12$ symmetry applied.

Jamieson etal, *EMBO J* **21** (2003) 3927

Atomic force microscopy

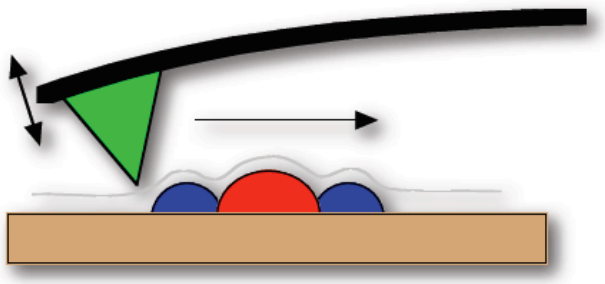

Scan membrane with proteins
(in physiological conditions)
=> protein arrangement (coarse view)
=> protein shape (high resolution)

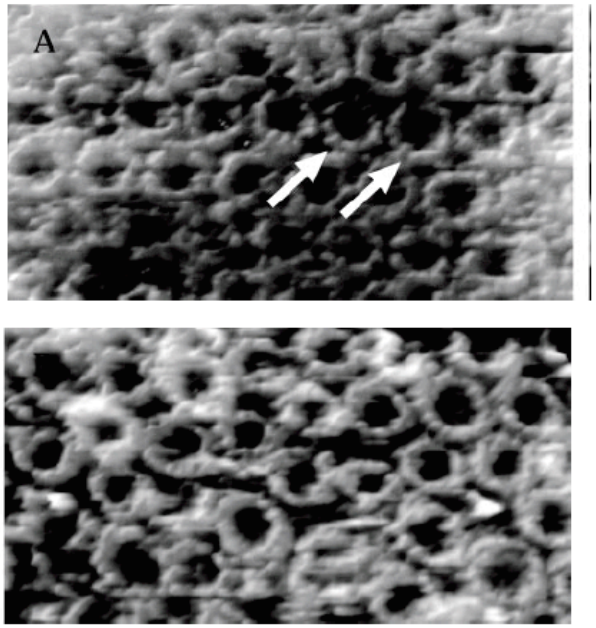

Shapes and sizes of monomeric
LH1 from purple bacteria

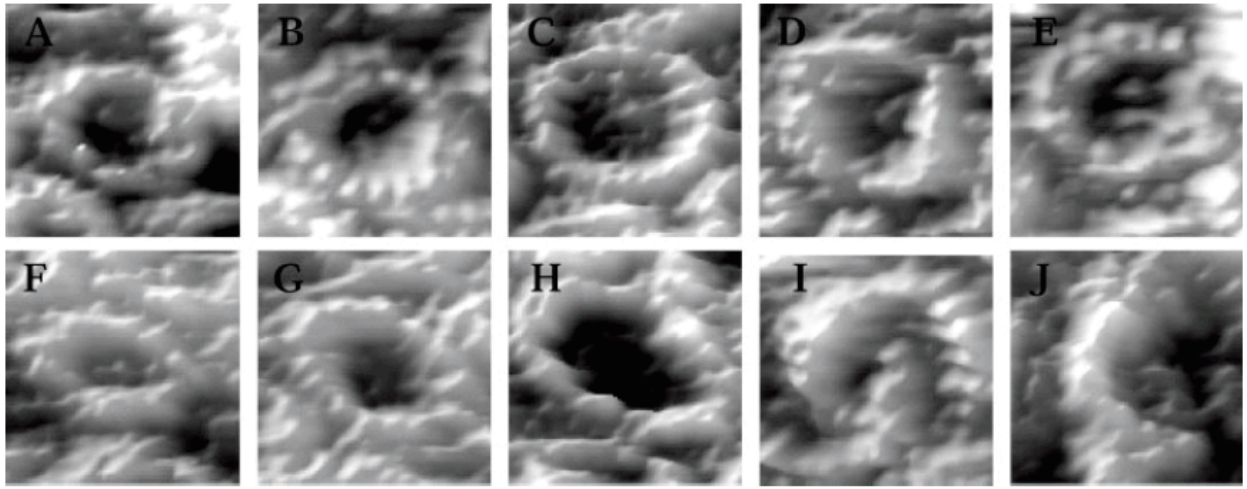

Bahatyrova etal, *J Biol Chem* **279** (2004) 21327

AFM pulling

Mechanical Unfolding of a Titin Ig Domain: Structure of Unfolding Intermediate Revealed by Combining AFM, Molecular Dynamics Simulations, NMR and Protein Engineering

Susan B. Fowler[1], Robert B. Best[1], José L. Toca Herrera[1]
Trevor J. Rutherford[1], Annette Steward[1], Emanuele Paci[2]
Martin Karplus[2,3] and Jane Clarke[1*]

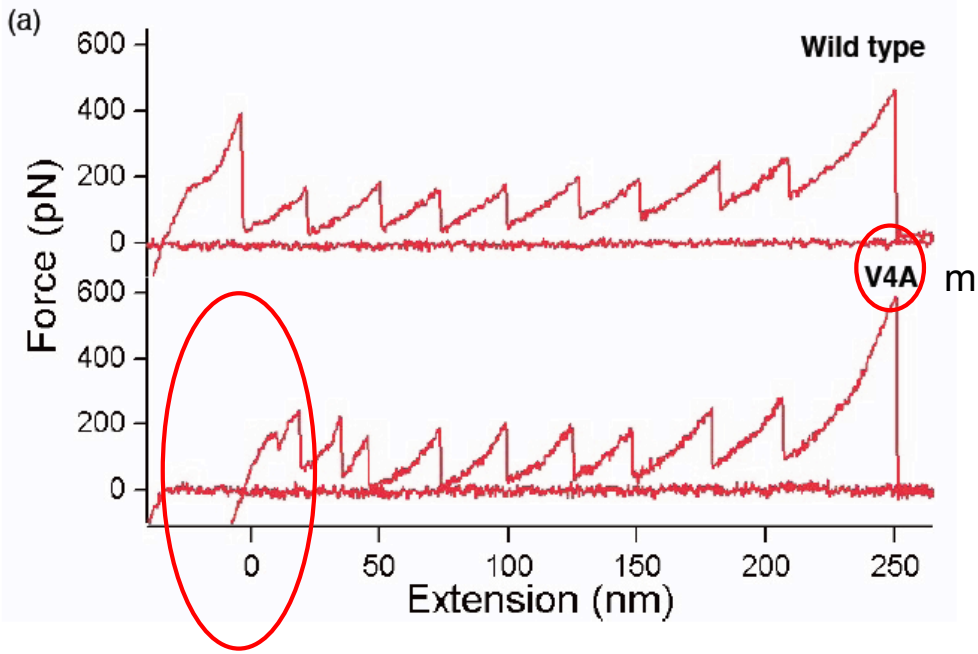

Can also be applied to protein complexes

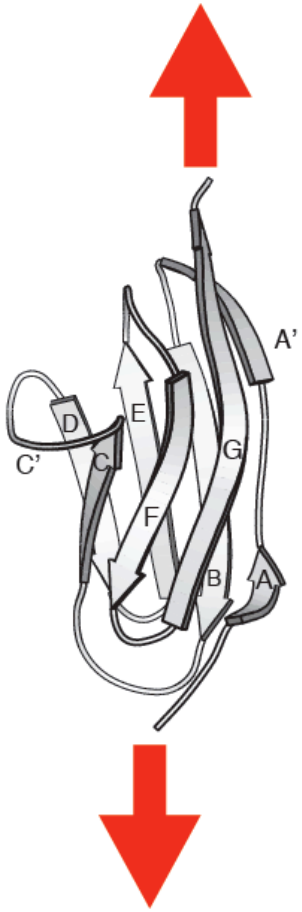

J. Mol. Biol. **322** (2002) 841–849

2.3.6 Fluorescence energy transfer

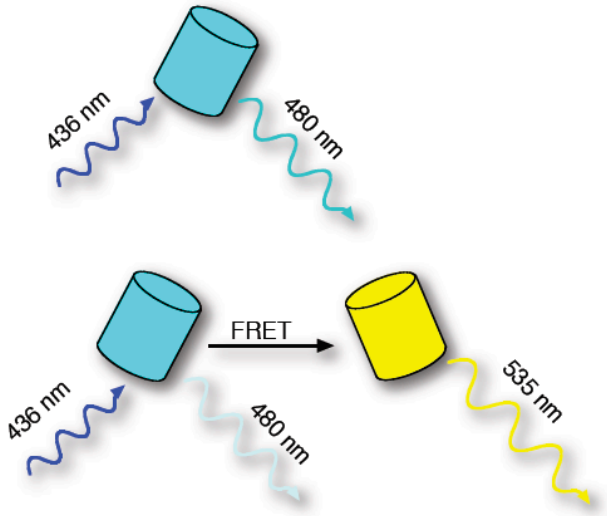

Chromophore of the cyan flourescent protein (CFP) absorbs at 436 nm and emits at 480 nm, YFP absorbs at 480 nm and emits at 535 nm.
=> **resonant** (non-radiative) energy **transfer** from CFP onto YFP when both are close enough

Resonant Förster transfer $\propto d^{-6}$

Tag two potential **complex partners** with CFP and YFP and measure **flourescence spectrum**:

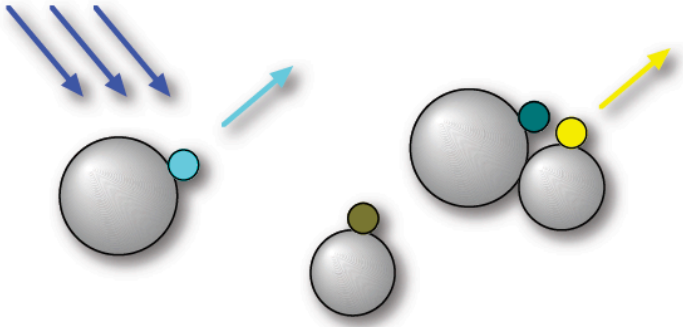

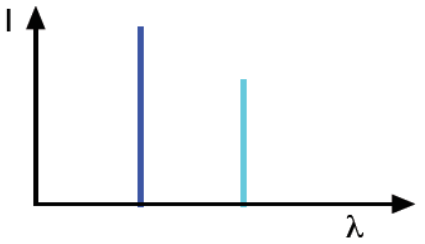

Observed when CFP and YFP are far away

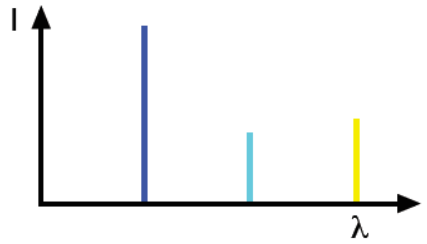

Observed when CFP and YFP are close

Structural techniques - overview

	X-ray crystallography	NMR	EM/ tomography	AFM	FRET	Y2H	TAP	MS
Structure ≤ 3Å	X	X	X					
structure ≥ 3Å	X	X	X	X				
contacts	X	X	X		X	X	X	X
proximity	X	X	X		X	X		
stoichiometry	X	X					X	X
complex symmetry	X	X	X	X				

Thanks to improvements
in EM detectors

2.4 Fitting atomistic structures into EM maps

Atomistic structure of
a part of the complex

Coarse EM structure of
the whole complex

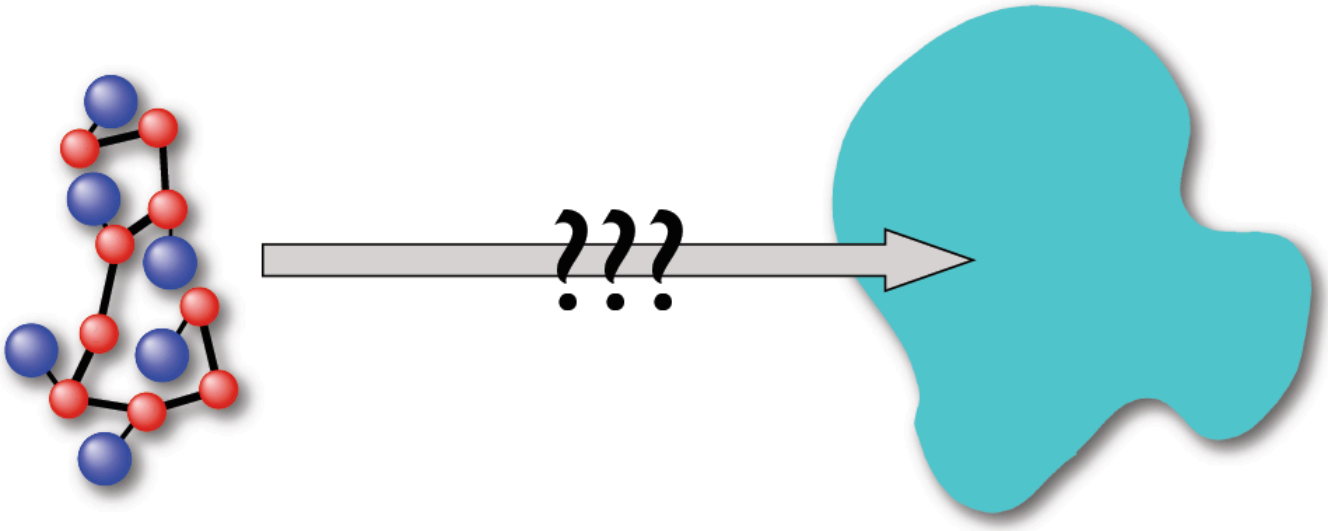

- same resolution for both structures
- exhaustive search with scoring
- choose best pose(s)

The procedure

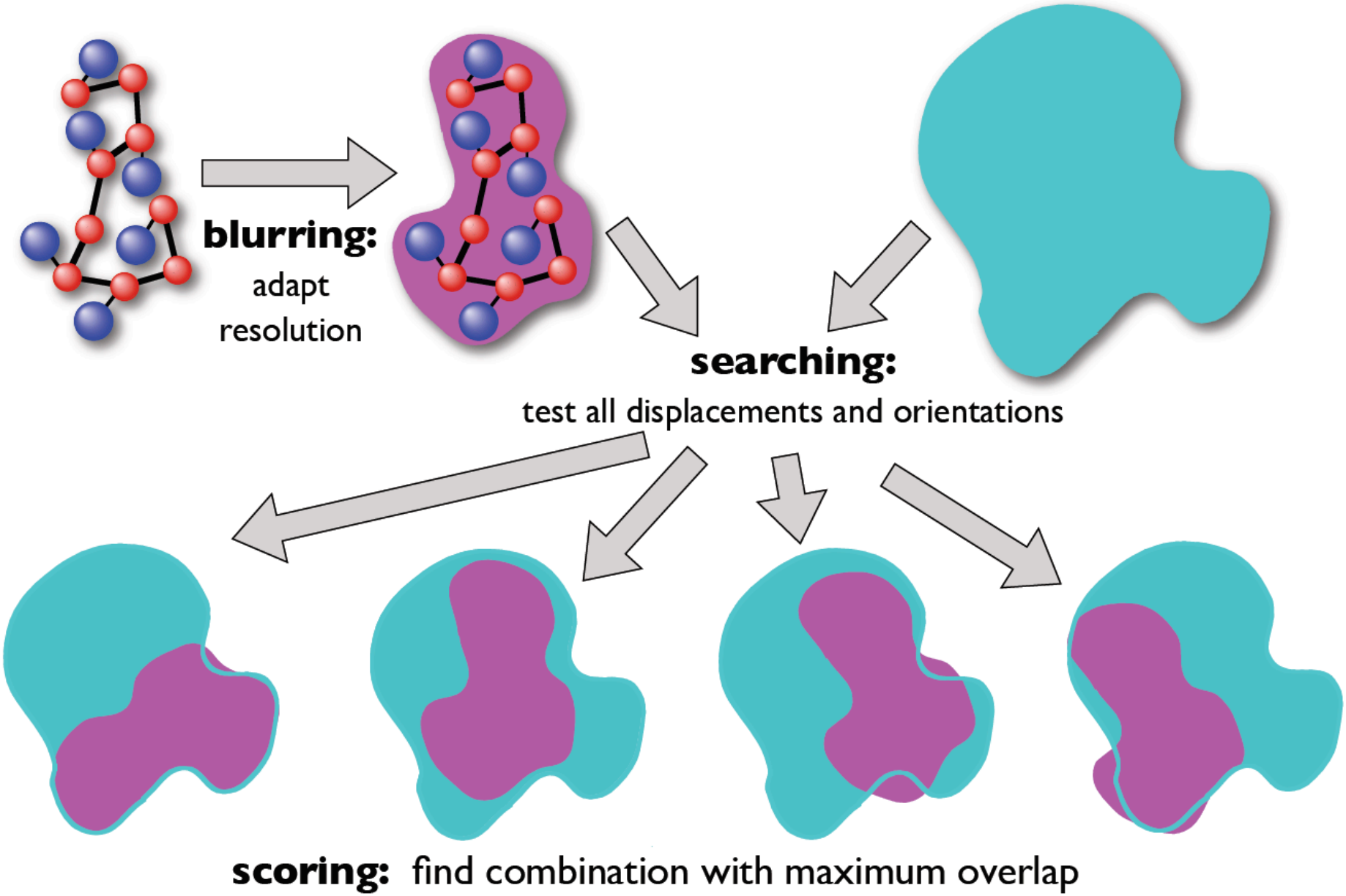

Step 1: blurring the picture

Mathematically:
convolution of (exact) atomistic structure f(x)
with experimental resolution g(x)

$$\tilde{f}(x) = (f \otimes g)(x) = \int dz\, f(z)\, g(x-z)$$

original data seen through the imaging apparatus

original signal

"kernel" => what is the image of a single point? (=delta signal)

Often: blurring with gaussian

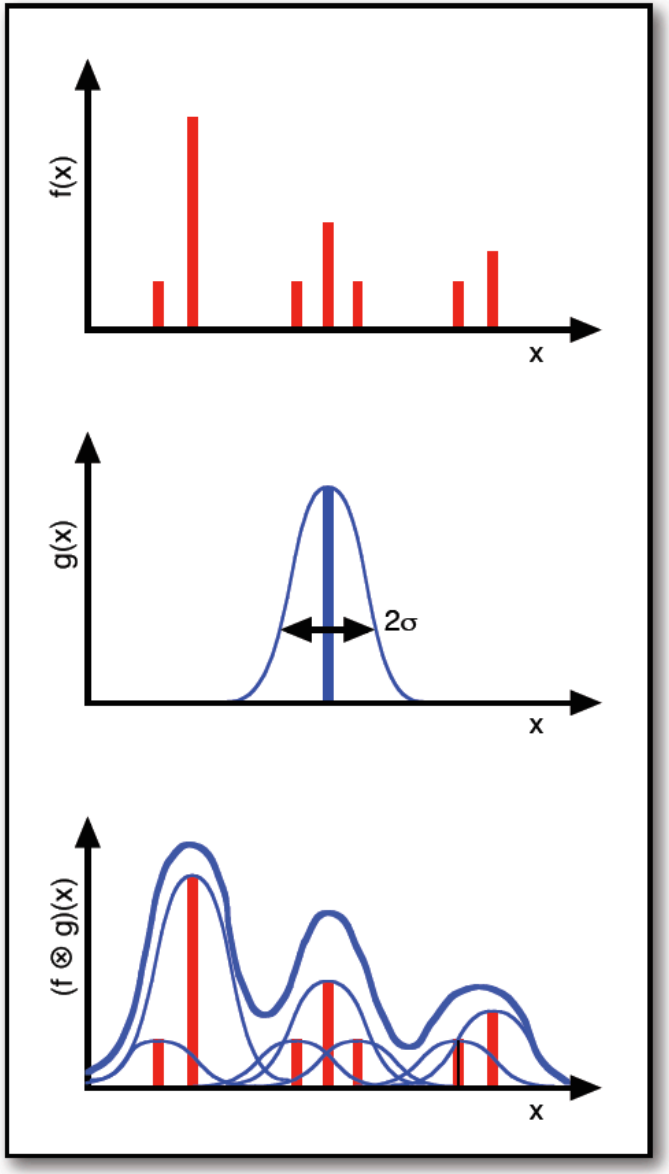

Put it on a grid

Discretize:

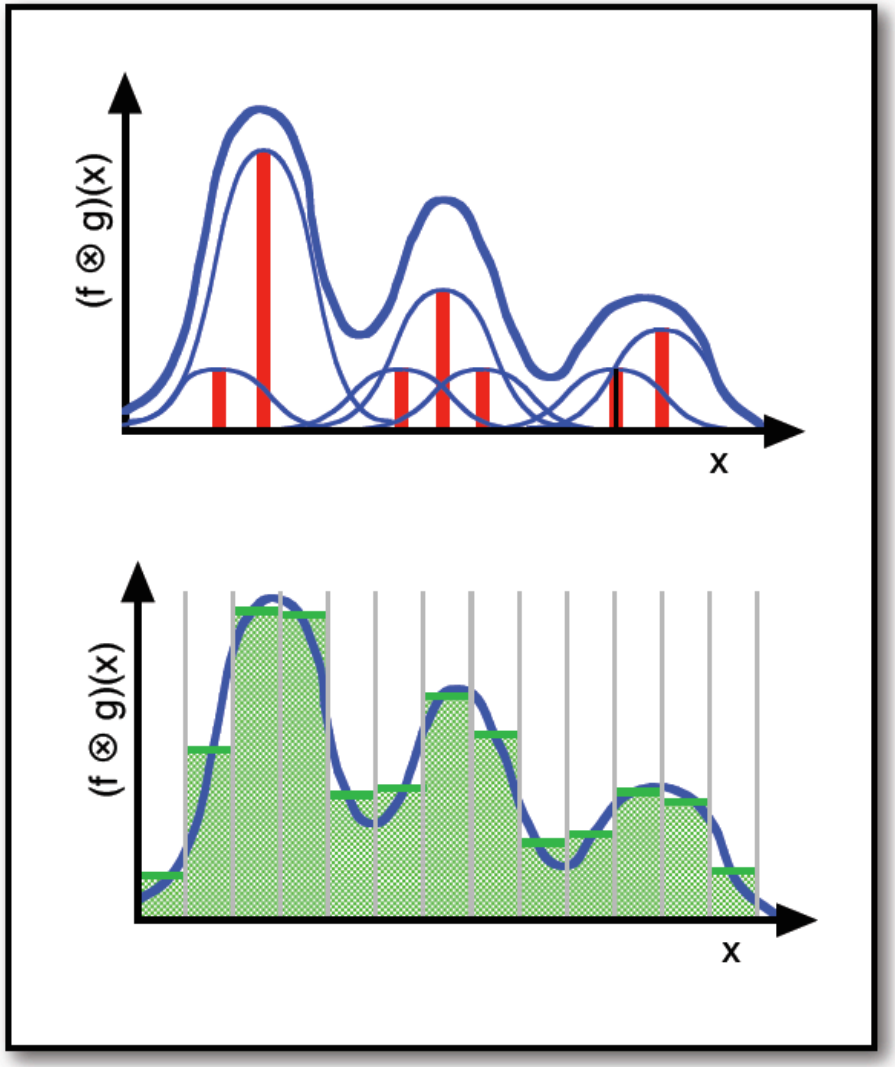

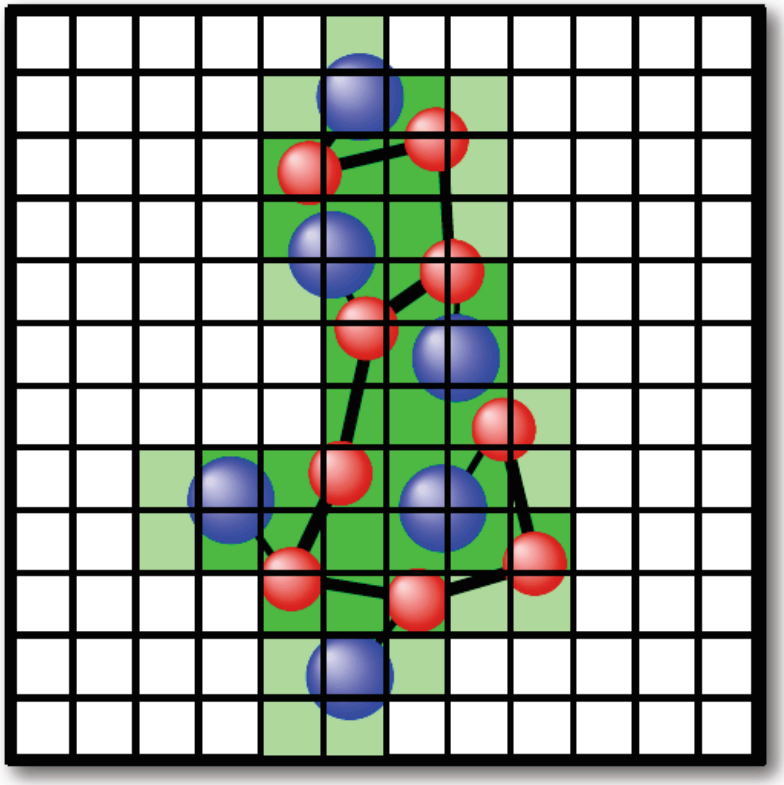

2.5 Fourier Transformation

Forward

$$F(k) = \int_{-\infty}^{\infty} dx\, e^{-ikx}\, f(x)$$

and inverse Fourier transform

$$f(x) = \frac{1}{2\pi} \int_{-\infty}^{\infty} dk\, e^{ikx}\, F(k)$$

with $$e^{ikx} = \cos(kx) + i \sin(kx)$$

=> convert between real and frequency (Fourier) space

short distances <=> high frequencies

long distances <=> low frequencies

Shift of the Argument

$$
\begin{aligned}
FT[f(x+\Delta x)] &= \int_{-\infty}^{\infty} dx\, e^{-ikx}\, f(x+\Delta x) \\
&= \int dy\, e^{-ik(y-\Delta x)}\, f(y) \\
&= e^{ik\,\Delta x} \int dy\, e^{-iky}\, f(y) \\
&= e^{ik\,\Delta x}\, FT[f(x)]
\end{aligned}
$$

Variable transformation:
$y = x + \Delta x$

change name of integration variable back from y to x

Convolution

$$\tilde{f}(x) = (f \otimes g)(x) = \int dz\, f(z)\, g(x-z)$$

Apply FT on both sides:

$$FT[\tilde{f}(x)] = FT[(f \otimes g)(x)] =$$

$$=$$

$$=$$

$$= FT[f(x)]\ FT[g(x)]$$

Integration in real space is replaced by simple multiplication in Fourier space.

But FTs need to be computed.

What is more efficient?

If the same width g(x) is used for multiple displaced datasets
=> do FT[g(x)] only once

Fourier on a Grid

On a finite grid: => maximum wavelength = length of grid
=> minimum wavelength = grid spacing
=> sum instead of integral

$$F_k = \sum_{j=0}^{N-1} e^{-2i\pi\, j\, k/N}\, f_j \qquad f_k = \frac{1}{N} \sum_{j=0}^{N-1} e^{+2i\pi\, j\, k/N}\, F_j$$

2.5.5 FFT by Danielson and Lanczos (1942)

Danielson and Lanczos showed that a discrete Fourier transform of length *N* can be rewritten as the sum of two discrete Fourier transforms, each of length *N/2.*

One of the two is formed from the even-numbered points of the original *N*, the other from the odd-numbered points.

F_k^e : *k*-th component of the Fourier transform of length *N/2* formed from the even components of the original f_j 's

F_k^o : *k*-th component of the Fourier transform of length *N/2* formed from the odd components of the original f_j 's

$$
\begin{aligned}
F_k &= \sum_{j=0}^{N-1} e^{-2\pi i k \frac{j}{N}} f_j \\
&= \sum_{j=0}^{\frac{N}{2}-1} e^{-2\pi i k \frac{2j}{N}} f_{2j} + \sum_{j=0}^{\frac{N}{2}-1} e^{-2\pi i k \frac{2j+1}{N}} f_{2j+1} \\
&= \sum_{j=0}^{\frac{N}{2}-1} e^{-2\pi i k \frac{j}{\frac{N}{2}}} f_{2j} + e^{-2\pi i k \frac{1}{N}} \sum_{j=0}^{\frac{N}{2}-1} e^{-2\pi i k \frac{j}{\frac{N}{2}}} f_{2j+1} \\
&= F_k^e + e^{-2\pi i k \frac{1}{N}} F_k^o
\end{aligned}
$$

FFT by Danielson and Lanczos (1942)

The wonderful property of the Danielson-Lanczos-Lemma is that it can be used recursively.

Having reduced the problem of computing F_k to that of computing F_k^e and F_k^o , we can do the same reduction of F_k^e to the problem of computing the transform of **its** *N/4* even-numbered input data and *N/4* odd-numbered data.

We can continue applying the DL-Lemma until we have subdivided the data all the way down to transforms of length 1.

What is the Fourier transform of length one? It is just the identity operation that copies its one input number into its one output slot.

For every pattern of $\log_2 N$ e‘s and o‘s, there is a one-point transform that is just one of the input numbers f_n

$$F_k^{eoeeoeo\ldots oee} = f_n \qquad \text{for some } n$$

FFT by Danielson and Lanczos (1942)

The next trick is to figure out which value of *n* corresponds to which pattern of e's and o's in $F_k^{eoeeoeo\ldots oee} = f_n$

Answer: reverse the pattern of e's and o's, then let e = 0 and o = 1,
and you will have, in binary the value of n.

This works because the successive subdividisions of the data into even and odd are tests of successive low-order (least significant) bits of *n*.

Thus, computing a FFT can be done efficiently in O(N log(N)) time.

Discretization and Convolution

For practical applications:
=> first put atomistic data onto the grid, then blur with FFT

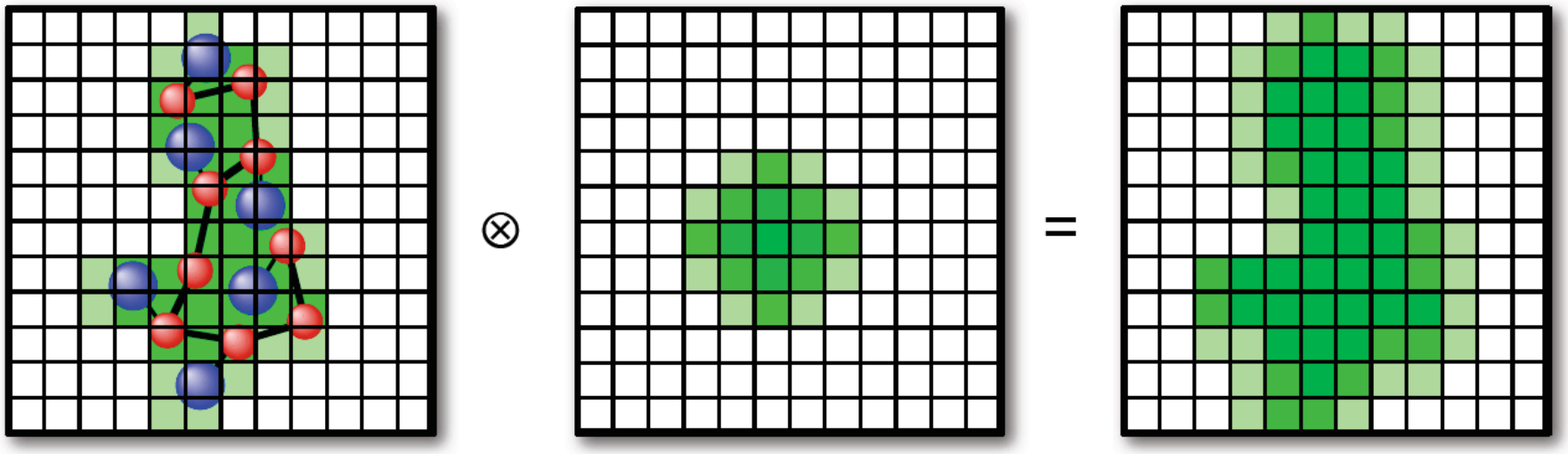

discretized hi-res data ⊗ blurring kernel = low-res image

Step 3: Scoring the Overlap

Most simple case:

- apply density threshold and count overlapping voxels
- displace images relative to each other, recount

=> find displacement with maximum overlap

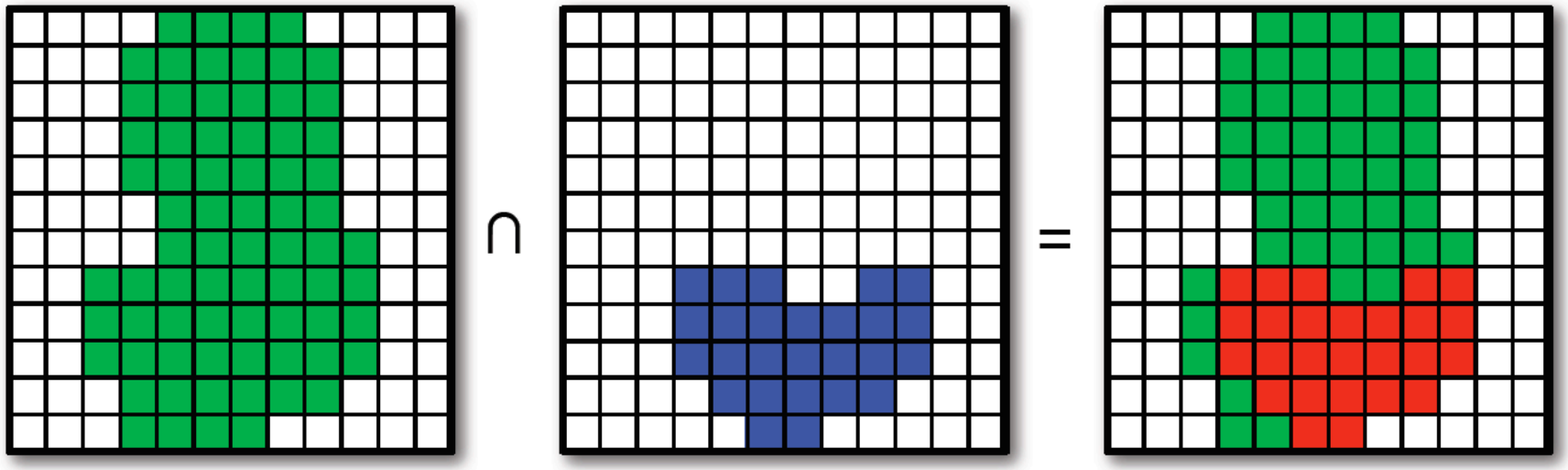

In matrix form with displacements x, y:

$$c(x,y) = \sum_{l=1}^{N} \sum_{m=1}^{N} a_{l,m}\, b_{l+x,m+y}$$

Cross Correlation

Generalization: maximize cross correlation of grided densities with respect to displacement (and orientation)

$$C_{x,y,z} = \sum_{l=1}^{N} \sum_{m=1}^{N} \sum_{n=1}^{N} a_{l,m,n} \times b_{l+x,m+y,n+z}$$

Note: maximize the cross-correlation <=> minimize the squared difference

On a grid with N^3 gridpoints => N^3 possible displacements
=> runtime $O(N^6)$

Further complication: the convolution

$$C_{x,y,z} = \sum_{l=1}^{N} \sum_{m=1}^{N} \sum_{n=1}^{N} a_{l,m,n} \times (g \otimes b_{l+x,m+y,n+z})$$

Correlation and Fourier

Apply Fourier transformation to both sides of

$$C_{x,y,z} = \sum_{l=1}^{N} \sum_{m=1}^{N} \sum_{n=1}^{N} a_{l,m,n} \times b_{l+x,m+y,n+z}$$

=> matrix multiplication

$$FT[C] = FT[A]^* \times FT[B]$$

Runtime of 3D FFT = $O(N^3 \log^3(N)) << N^6$
=> all possible displacements tested simultaneously

Note: FT[A] only calculated once initially
=> two FFTs per orientation
=> scan orientation via Euler angles

<== Step 2: exhaustive search

Include convolution

Maximize

$$C_{x,y,z} = \sum_{l=1}^{N} \sum_{m=1}^{N} \sum_{n=1}^{N} a_{l,m,n} \times (g \otimes b_{l+x,m+y,n+z})$$

In Fourier space:

Insert convolution $FT[f \otimes g] = FT[f] \times FT[g]$

Into correlation:

$$\begin{aligned} FT[C] &= FT[A]^* \times FT[G \otimes B] \\ &= FT[A]^* \times (FT[G] \times FT[B]) \\ &= (FT[A]^* \times FT[G]) \times FT[B] \end{aligned}$$

can be precomputed

2 FFTs + 1 matrix multiplication

2.7 Katchalski-Kazir algorithm

Proc. Natl. Acad. Sci. USA
Vol. 89, pp. 2195–2199, March 1992
Biophysics

Molecular surface recognition: Determination of geometric fit between proteins and their ligands by correlation techniques

(protein–protein interaction/surface complementarity/macromolecular complex prediction/molecular docking)

EPHRAIM KATCHALSKI-KATZIR[†‡], ISAAC SHARIV[§], MIRIAM EISENSTEIN[¶], ASHER A. FRIESEM[§], CLAUDE AFLALO[‖], AND ILYA A. VAKSER[†]

Departments of [†]Membrane Research and Biophysics, [§]Electronics, [¶]Structural Biology, and [‖]Biochemistry, Weizmann Institute of Science, Rehovot 76100, Israel

Contributed by Ephraim Katchalski-Katzir, October 24, 1991

Developed for protein-ligand docking
<=> same techniques applicable for docking "on the inside"

Discretization for docking

Next, to distinguish between the surface and the interior of each molecule, we retain the value of 1 for the grid points along a thin surface layer only and assign other values to the internal grid points. The resulting functions thus become

$$\bar{a}_{l,m,n} = \begin{cases} 1 & \text{on the surface of the molecule} \\ \rho & \text{inside the molecule} \\ 0 & \text{outside the molecule,} \end{cases} \qquad [2a]$$

and

$$\bar{b}_{l,m,n} = \begin{cases} 1 & \text{on the surface of the molecule} \\ \delta & \text{inside the molecule} \\ 0 & \text{outside the molecule,} \end{cases} \qquad [2b]$$

where the surface is defined here as a boundary layer of finite width between the inside and the outside of the molecule. The parameters ρ and δ describe the value of the points inside the molecules, and all points outside are set to zero. Two-

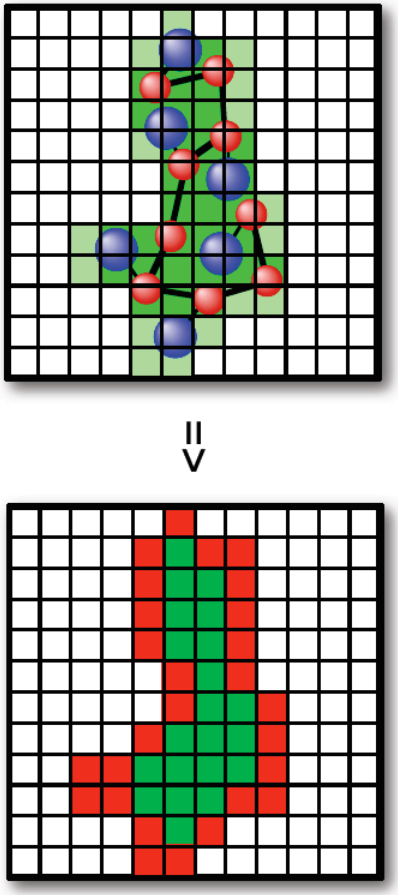

Typical values: $\rho = -15$, $\delta = 1$

=> penalty for overlap of volumes

Docking the hemoglobin dimer

2D cross sections at I = 46 (N = 90)

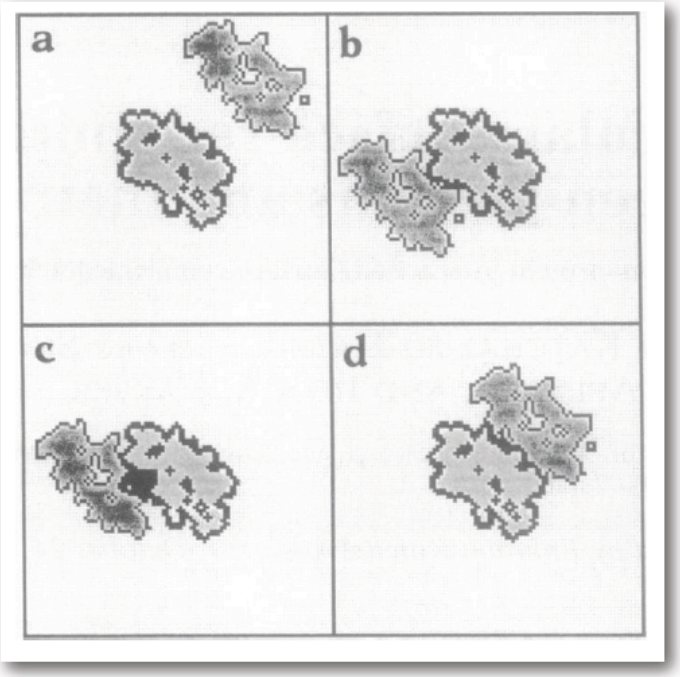

a) no contact
b) limited contact
c) overlap (black area)
d) good geometric match

Correlation at α = 0

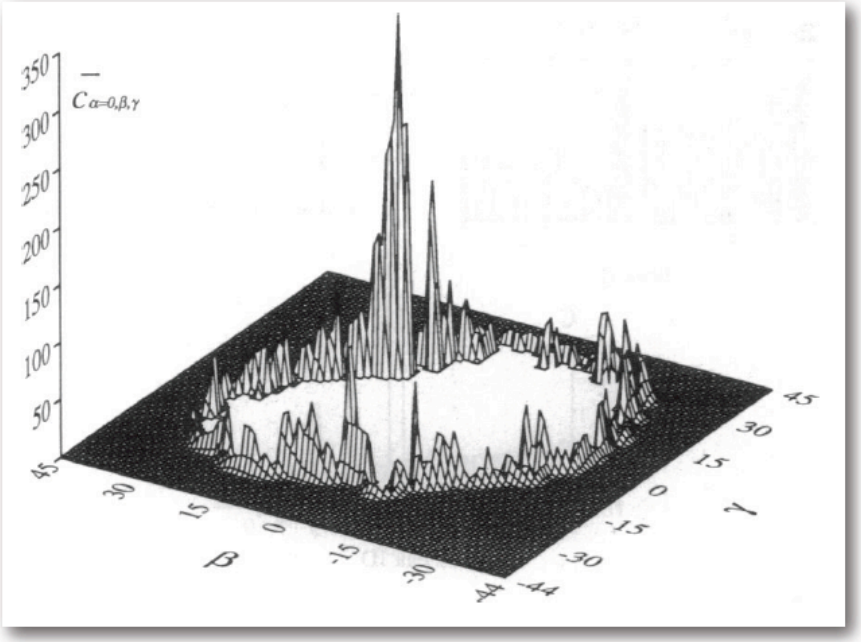

highest peak corresponds to native dimer arrangement

The algorithm

The entire procedure described above can be summarized by the following steps:
(*i*) derive $\bar{a}$ from atomic coordinates of molecule **a** (Eq. **2**),
(*ii*) $A^* = [\mathrm{DFT}(\bar{a})]^*$ (Eq. **4**),
(*iii*) derive $\bar{b}$ from atomic coordinates of molecule **b** (Eq. **2**),
(*iv*) $B = \mathrm{DFT}(\bar{b})$ (Eq. **4**),
(*v*) $C = A^* \cdot B$ (Eq. **5**),
(*vi*) $\bar{c} = \mathrm{IFT}(C)$ (Eq. **6**),
(*vii*) look for a sharp positive peak of $\bar{c}$,
(*viii*) rotate molecule **b** to a new orientation,
(*ix*) repeat steps *iii–viii* and end when the orientations scan is completed, and
(*x*) sort all of the peaks by their height.

Each high and sharp peak found by this procedure indicates geometric match and thus represents a potential complex. The relative position and orientation of the molecules within each such complex can readily be derived from the

Katchalski-Kazir et al. 1992

Algorithm has become a workhorse for docking and density fitting.

Problem I: limited contrast

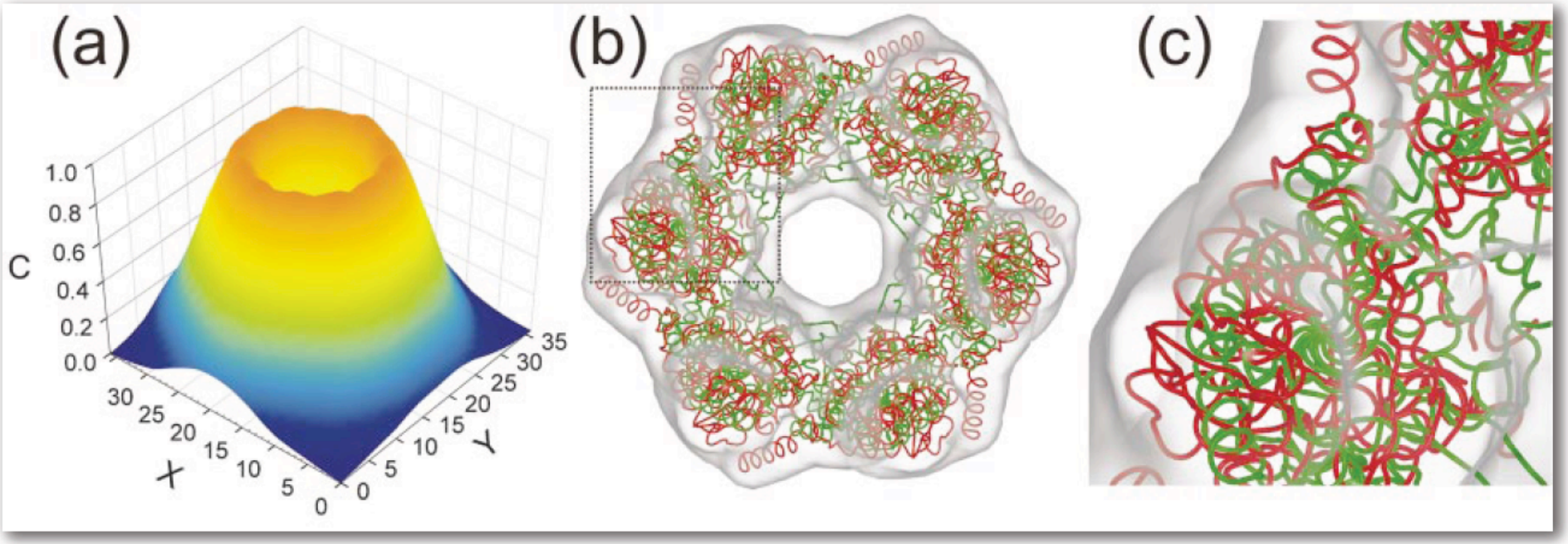

Docking of the RecA helicase monomer into simulated EM density of the hexamer at 15 Å resolution
(exhaustive 6D search with 5Å / 9° steps plus off-lattice optimization)
=> multiple fits with similar correlations

Chacón, Wriggers, *J. Mol. Biol.* **317** (2002) 375

2.6 Laplace filter

Evaluate $$\nabla^2 = \frac{d^2}{dx^2} + \frac{d^2}{dy^2} + \frac{d^2}{dz^2}$$

on a grid: $$\nabla^2 a_{l,m,n} = -6a_{l,m,n} + a_{l+1,m,n} + a_{l-1,m,n} + a_{l,m+1,n} + a_{l,m-1,n} + a_{l,m,n+1} + a_{l,m,n-1}$$

Correlation:

$$C_{x,y,z} = \sum_{l=1}^{N} \sum_{m=1}^{N} \sum_{n=1}^{N} (\nabla^2 \otimes a_{l,m,n}) \times (\nabla^2 \otimes g \otimes b_{l+x,m+y,n+z})$$

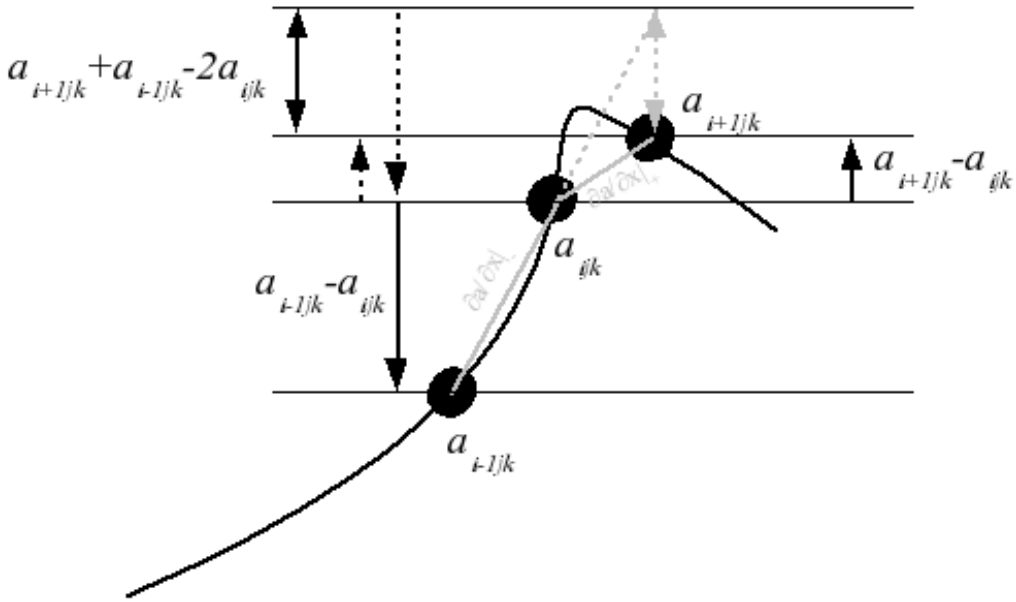

Enhanced contrast ➔ better fit

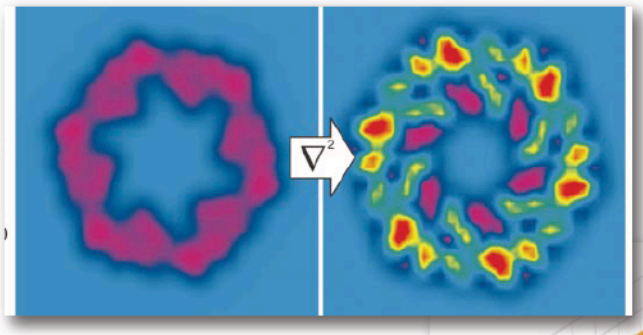

With the density alone:

With the Laplacian filter:

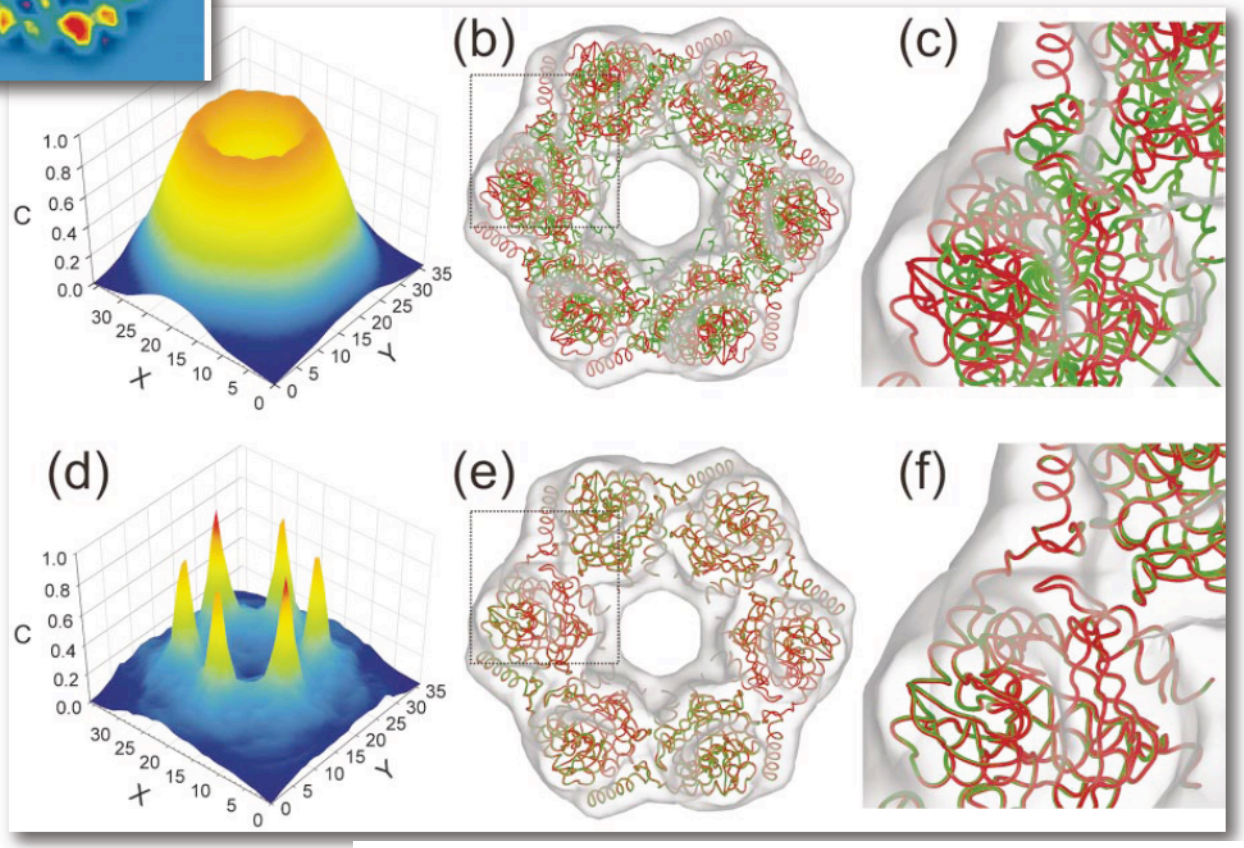

Chacón, Wriggers, *J. Mol. Biol.* **317** (2002) 375

The big picture

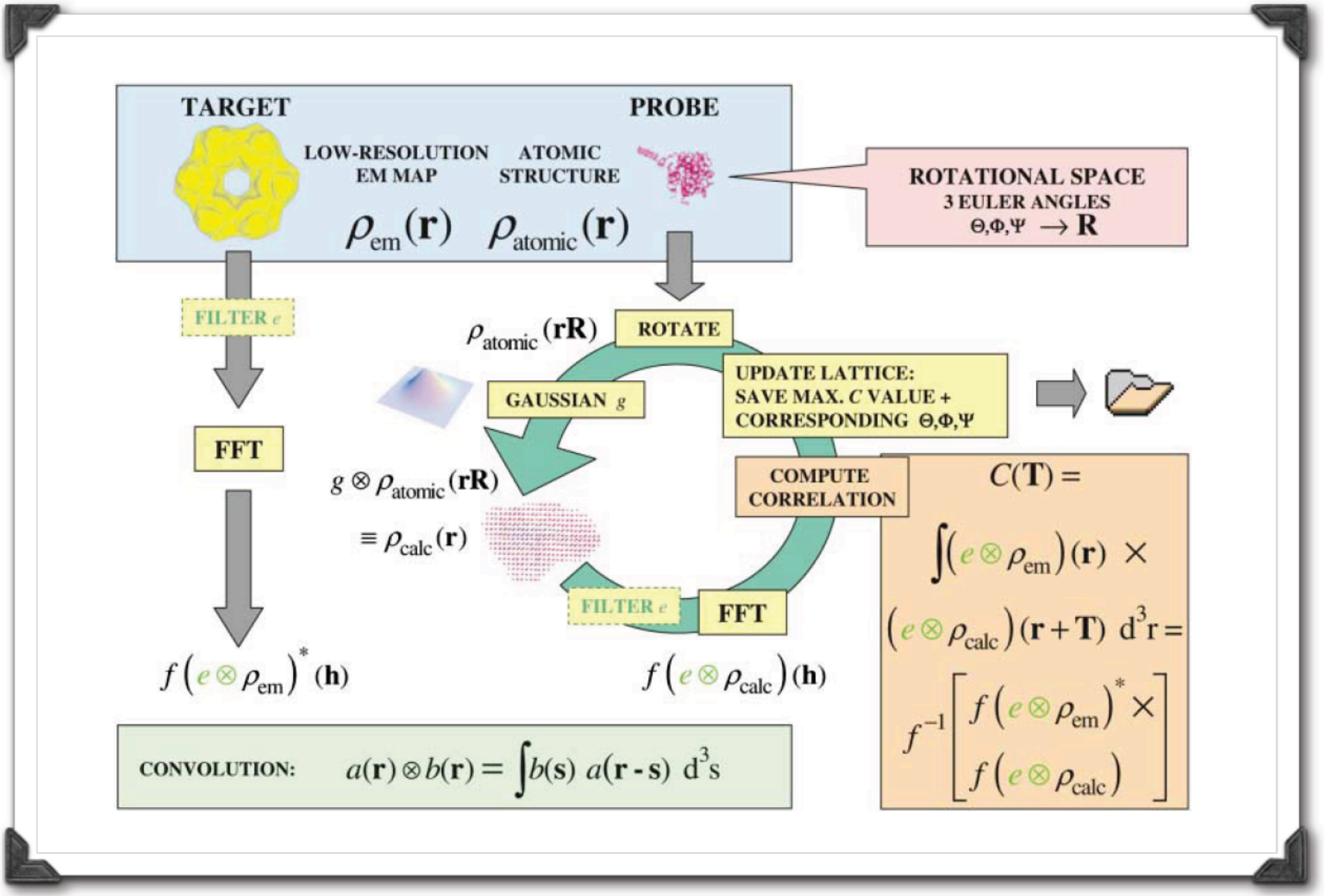

Wriggers, Chacón, *Structure* **9** (2001) 779

Problem 2: more efficient search

BIOINFORMATICS ORIGINAL PAPER

Vol. 23 no. 4 2007, pages 427–433
doi:10.1093/bioinformatics/btl625

Structural bioinformatics

ADP_EM: fast exhaustive multi-resolution docking for high-throughput coverage

José Ignacio Garzón, Julio Kovacs[1], Ruben Abagyan[1] and Pablo Chacón*

Centro de Investigaciones Biológicas, CSIC, Ramiro de Maeztu 9, 28040 Madrid, Spain and
[1]Department of Molecular Biology, The Scripps Research Institute La Jolla, CA 92037, USA

Received on September 28, 2006; revised on November 28, 2006; accepted on December 4, 2006
Advance Access publication December 6, 2006
Associate Editor: Alex Bateman

Observations:

- many displacements can be excluded a priori (FFT alg. calculates them all)
- FFT idea makes more sense for rotations (no simple limit on rotations)

Masked displacements

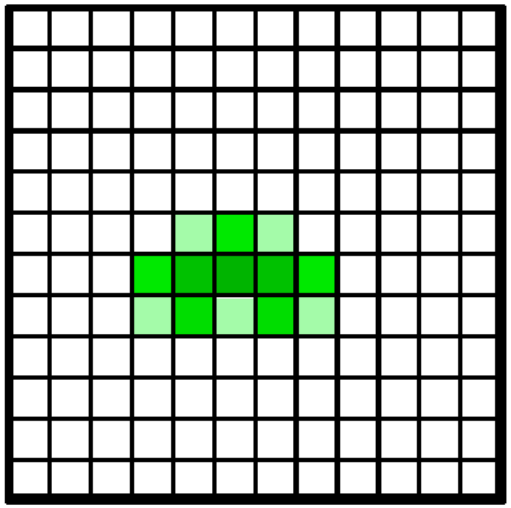

Probe

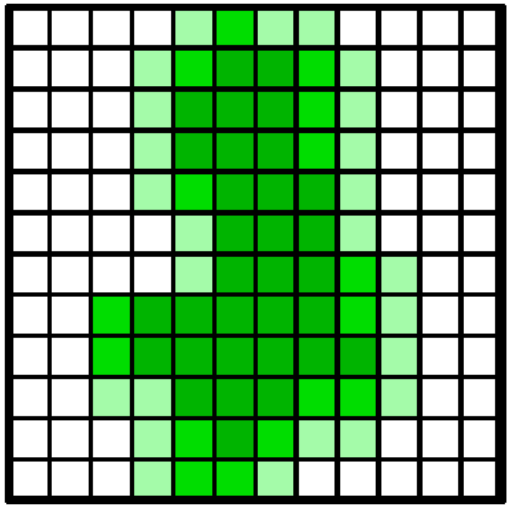

Target

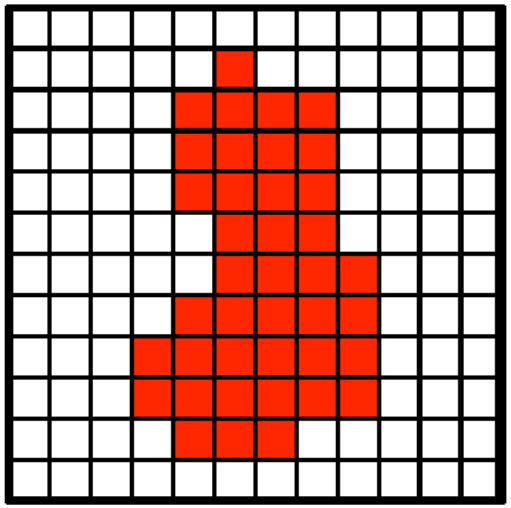

Mask =
potential hits

Search space for displacements =
(inside of the target molecule) – (extent of the probe)

Rotational search

Express densities in spherical harmonics on "onion shells"

$$\rho_{\mathrm{low}}(r,\beta,\lambda) = \sum_{l=0}^{B-1} \sum_{m=-l}^{l} C_{lm}^{\mathrm{low}}(r) Y_{lm}(\beta,\lambda) \qquad \rho_{\mathrm{high}}(r,\beta,\lambda) = \sum_{l=0}^{B-1} \sum_{m=-l}^{l} C_{lm}^{\mathrm{high}}(r) Y_{lm}(\beta,\lambda),$$

Y_{lm}	l = 0	l = 1	l = 2	l = 3
m = -3				$\sqrt{\frac{35}{64\pi}}\sin^3\vartheta\, e^{-3i\varphi}$
m = -2			$\sqrt{\frac{15}{32\pi}}\sin^2\vartheta\, e^{-2i\varphi}$	$\sqrt{\frac{105}{32\pi}}\sin^2\vartheta\cos\vartheta\, e^{-2i\varphi}$
m = -1		$\sqrt{\frac{3}{8\pi}}\sin\vartheta\, e^{-i\varphi}$	$\sqrt{\frac{15}{8\pi}}\sin\vartheta\,\cos\vartheta\, e^{-i\varphi}$	$\sqrt{\frac{21}{64\pi}}\sin\vartheta\,(5\cos^2\vartheta-1)\, e^{-i\varphi}$
m = 0	$\sqrt{\frac{1}{4\pi}}$	$\sqrt{\frac{3}{4\pi}}\cos\vartheta$	$\sqrt{\frac{5}{16\pi}}(3\cos^2\vartheta-1)$	$\sqrt{\frac{7}{16\pi}}(5\cos^3\vartheta-3\cos\vartheta)$
m = 1		$-\sqrt{\frac{3}{8\pi}}\sin\vartheta\, e^{i\varphi}$	$-\sqrt{\frac{15}{8\pi}}\sin\vartheta\,\cos\vartheta\, e^{i\varphi}$	$-\sqrt{\frac{21}{64\pi}}\sin\vartheta\,(5\cos^2\vartheta-1)\, e^{i\varphi}$
m = 2			$\sqrt{\frac{15}{32\pi}}\sin^2\vartheta\, e^{2i\varphi}$	$\sqrt{\frac{105}{32\pi}}\sin^2\vartheta\cos\vartheta\, e^{2i\varphi}$
m = 3				$-\sqrt{\frac{35}{64\pi}}\sin^3\vartheta\, e^{3i\varphi}$

Correlation for **all orientations** at a given displacement:

$$C(R) = FT^{-1}_{m,h,m'}\left[\sum_{l} d^l_{mh}\; d^l_{hm'} \int_0^{\infty} C_{lm}^{\mathrm{low}}(r)\overline{C_{lm'}^{\mathrm{high}}(r)} r^2 dr\right]$$

Known Fourier coefficients of spherical harmonics Y_{lm}.

Accuracy

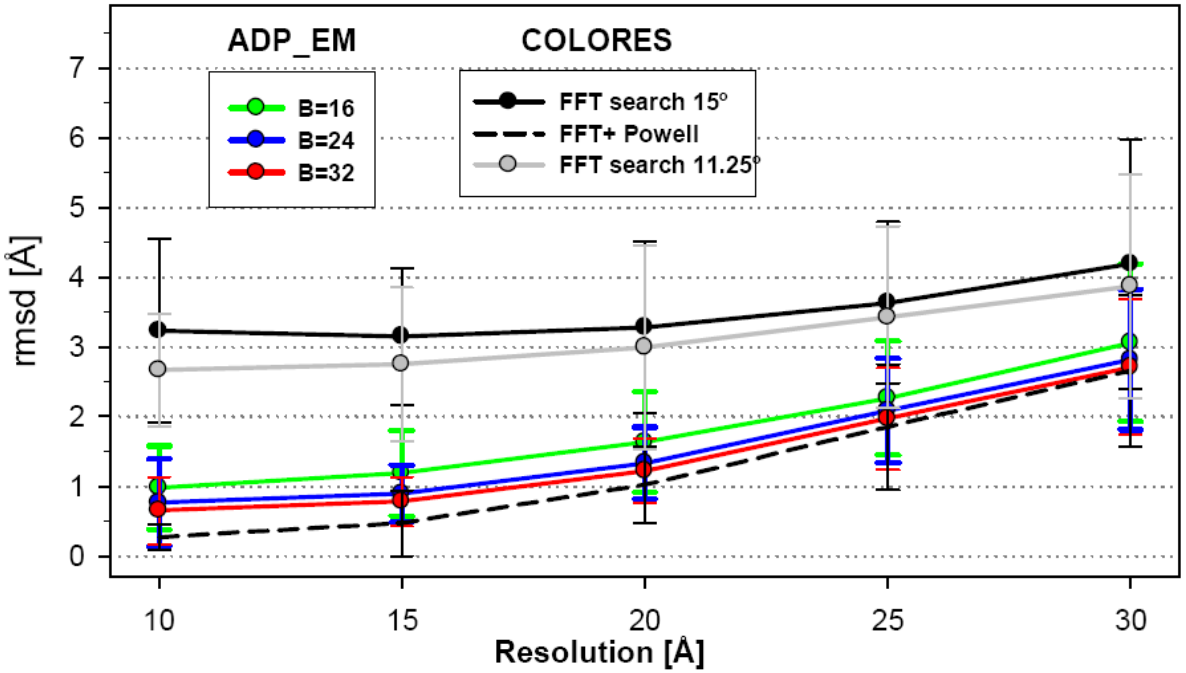

rmsd with respect to known atomistic structure of target.

Registration accuracy on simulated EM maps of 28 structures
for bandwidths (number of angular sampling points) of
B = 16, 24 32 (11°, 8°, ~ 6°)
compared to Wriggers' COLORES (situs package – Katchalski-Katzir algorithm + local Powell optimization)

Performance

Table 1. Timing results, in seconds, obtained with the benchmark described in Figure 1

	Sampling B/°	Resolution 10Å	15Å	20Å	25Å	30Å
ADP_EM	16/11°	28	31	35	34	38
	24/8°	100	108	119	118	123
	32/6°	226	220	225	216	221
FFT search	–/15°	1697	1926	2341	5028	6681
Powell minim	–/15°	375	918	1747	3739	6597

ADP_EM (Another Docking Platform for EM) is much faster

- only limited spatial region is scanned
- fast evaluation of the orientational correlation via FFT
- spherical harmonics allow for better rotational representation
  => higher accuracy

Some examples

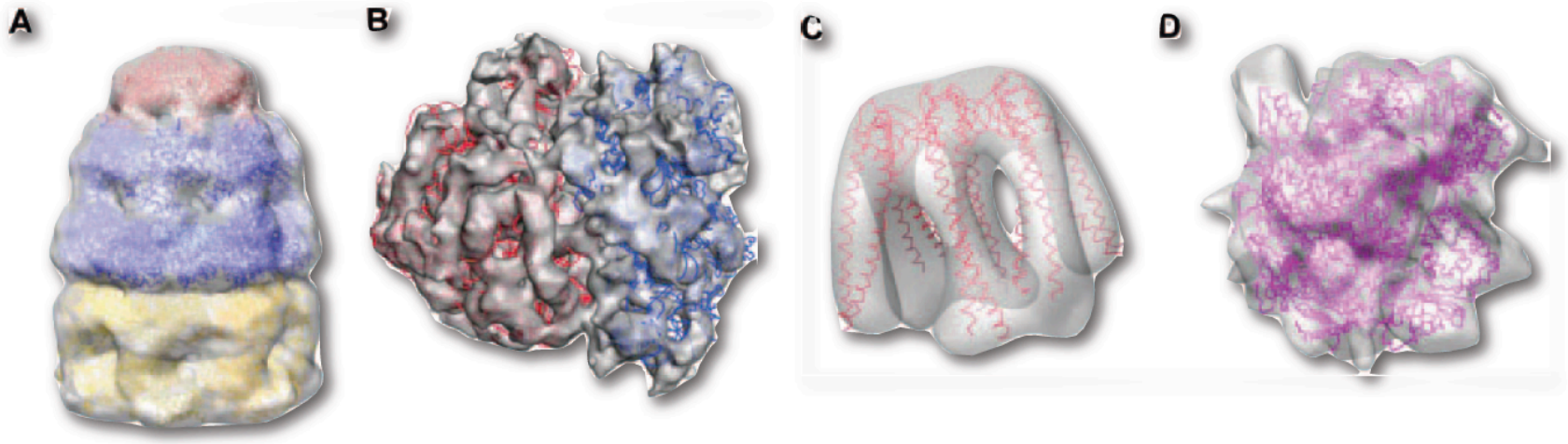

Fig. 2. Docking results with experimental EM data. (**A**) *E.coli* GroES-ADP7-GroEL-ATP7 from *E.coli* at 23.5 Å (EMD ID 1046, PDB: 1ml5); ADP and ATP GroEL subunits have been docked independently to reconstruct the cis and trans heptameric rings of the complex. For GroES the whole heptamer was used. (**B**) Docking of 30S and 50S subunits into *E.coli* ribosome map at 14 Å (EMD ID 1046, PDB: 1gix/1giy). Single-molecule docking of prefoldin (**C**) at 23 Å (Martin-Benito *et al.*, 2002), PDB: 1l6h, and of yeast RNA polymerase II (**D**) at 15 Å (Craighead *et al.*, 2002), PDB: 1fxk.

Summary

Today:

Docking into EM maps

- Discretization
- Correlation and blurring via FFT => Katchalski-Katzir algorithm
- Laplace filter => enhances contrast
- ADP_EM: FFT for rotations, scan displacements => better performance

Next lecture V3:

Computational Methods to assemble higher-order protein complexes

Bioinformatic characterization of protein interfaces